UNIVERSITY OF CALIFORNIA
RIVERSIDE

Fire Behavior Modeling - Experiment on Surface Fire Transition to the Elevated Live Fuel

A Thesis submitted in partial satisfaction
of the requirements for the degree of

Master of Science

in

Mechanical Engineering

by

Sunday Omodan

March 2015

Thesis Committee:
Dr. Marko Princevac, Chairperson
Dr. Guillermo Aguilar
Dr. Masaru P. Rao

The Thesis of Sunday Omodan is approved:

_____

_____

_____
Committee Chairperson

University of California, Riverside

Acknowledgement

A number of people have provided me with help and support in completing this thesis.

In particular, I would like to thank:

- Prof. Marko Princevac, my supervisor for this dissertation, who greatly supported the idea of experimental element of the project and who provided advice and valuable comments in relation to the methodology and the content of the dissertation.
- Special thanks to my Thesis Committee Members, Dr. Marko Princevac (Committee Chairperson), Dr. Guillermo Aguilar (Department Chair) and Dr. Masaru P. Rao for sacrificing their precious times to grade this thesis defense.
- The graduate division, for their financial support through the Dean's prestigious fellowship award.
- The staff of the PSW Forest Service Research Station, Riverside, California laboratory and in particular Dr. David Weise, Ms. Gloria Burke, and Mr. Joey Chong who contributed enormously to the experimental part of this project.
- My research team from the Department of Mechanical Engineering, University of California, Riverside, most especially Christian Bartolome(PhD), Raul-Delga Delgadillo, Chirawat Sanpakit, Turner Bradshaw, Lyna Hakimi, Joel Malagon, and Ryan Torento who worked tirelessly to make the laboratory experiment a success.

- Mr. Chirawat Sanpakit (Chris) who did a tremendous job in the review of this thesis to make sure everything is error free.
- Finally, I would like to thank my wife Oluwaremi C. Omodan for her constant support and never-ending patience.

Dedication

This thesis is dedicated to my wife who has been a great source of motivation and inspiration all the way since the beginning of my studies.

Also, this thesis is dedicated to my Children, Emmanuel Omodan, John Omodan and Joseph Omodan who believe in the richness of learning from childhood.

ABSTRCT OF THE THESIS

Fire Behavior Modeling - Experiment on Surface
Fire Transition to the Elevated Live Fuel

by

Sunday Omodan

Master of Science, Graduate Program in Mechanical Engineering
University of California, Riverside, March 2015
Dr. Marko Princevac, Chairperson

Recent increase in the number of wildfires globally over the last decade has made fire behavior modelling a major subject of scientific concern. Although, there have been wildfire studies since the beginning of 19th century, and this effort is accelerating over the last decade, the behavior of wild fire still remains largely unknown. Using the State of California, United States as a case study, increase of wildland fires in wild-urban interface is alarming. There was an estimated 9,907 wildland fires claiming 577,675 acres and additional 542 prescribed fires used to treat 48,544 acres by various agencies in 2013. Fire behavior modeling and measurements can lead to tools for decision making in both combating wild fires and validating fire predictions. Earlier studies focused on coniferous forest crown fires but very little research has been conducted on chaparral crown fires. These elevated chaparral fuels approximately 1 foot from surface can be modeled as crown fires.

This thesis discusses the numerical simulation of fire behavior using Fire Dynamic Simulator (FDS) and laboratory experiments designed to model surface/crown fire behavior. FDS is a computational fluid dynamic (CFD) model that is developed to analyze

fire behavior under various conditions. The conditions in FDS were set as close as possible to match the laboratory experiments used. The observed variables were surface temperature, bulk density, fuel heights, wind, heights between fuel beds and hot spots. Laboratory experiment were conducted at the United States Department of Agriculture Forest Service Pacific Southwest (USDA FS PSW) Research Station. The experiments focused on understanding chaparral crown fire behavior, particularly the ignition, mechanisms of flame propagation, spreading, flame front velocity and fuel consumption rates. Impacts of surface fires on crown fuels were studied together with the effects of winds, humidity, environmental temperature and fuel moisture content.

Results from FDS were in qualitative agreement with laboratory experiments of surface fire. However, in numerical simulations crown would be ignited only when surface and elevated fuels are of the same kind. The analysis of this model behavior is out of the scope of this thesis and will be subject of future research.

Contents

List of Tables

List of Figures

Nomenclature

English

c	specific heat of the body
C	empirically derived constant
C_p	constant pressure specific heat
D	diffusion coefficient, fire diameter
D^*	characteristic fire diameter
H_o	HRR per unit mass of oxygen consumed
g	acceleration of gravity
h	enthalpy; heat transfer coefficient
I	radiation intensity
K	thermal conductivity, turbulent kinetic energy
L	flame height
m	mass of body
M_i	molecular weight of ith gas species
m_o'''	oxygen consumption rate
P	pressure
q_r	radiative heat flux vector
q'''	heat release rate per unit volume
Q^*	dimensionless HRR
Q	total heat release rate
Q_c	convective heat release rate
T	temperature
t	time
u	velocity

u	(u, v, w) velocity vector
W_i'''	production rate of ith species per unit volume
Y_F	mass fraction of fuel in the fuel stream
Y_i	mass fraction of ith species
Y_o	mass fraction of oxygen
∞	mass fraction of oxygen in ambient
z	height above fire base
Z	mixture fraction
Z_F	mixture fraction at flame surface
$Z_{F,eff}$	effective flame mixture fraction

Greek

δx	nominal grid size
ε	viscous dissipation energy
κ	absorption coefficient
μ	dynamic viscosity
ρ	density
σ	Stefan-Boltzmann constant
τ	viscous stress tensor
v_i	flame front velocity
χ_r	local radiative loss fraction

Acronyms

CFD Computational Fluid Dynamics

FDS Fire Dynamics Simulator

FS Forest Service

HoC Heat of Combustion

HRR Heat Release Rate

ISO International Standards Organization

LES Large Eddy Simulation

MISC Miscellaneous

MLR Mass Loss Rate

NIST National Institute of Standards and Technology

PSW Pacific South West

RTE Radiative Transport Equation

TC Thermocouple

USDA United States Department of Agriculture

1.0 Introduction

Predicting the potential behavior and effects of wildland fire is an essential task in fire management (Scott et al., 2005). In the first part of this thesis, a computational fluid dynamic (CFD) model is used to analyze fire behavior under certain boundary conditions. In the second part of the thesis, a new fire behavior modeling of surface and crown fires is conducted in a wind tunnel. The eventual goal of simplified laboratory experiments is to develop scaling criteria for application in wildland fire cases. In the presented work, the laboratory fire was used to validate the results of the numerical approach.

Due to the complex nature of wildfires most models (see review by Engstrom et al., 2010) are based on the empirical correlations put together by Byram (1959), Fosberg and Deeming (1971), Rothermel (1972), Van Wagner (1973) and Albini (1976). Some of these models are extensive and operational and suitable for use by fire managers. These models include FARSITE (Finney, 1998) and BEHAVE (Andrews, 1986). Empirical models consider certain parameters like quantity and type of fuel, wind, and slope and temperature as the controlling factor for fire spread in vegetation. Although, these models were considered to be accurate for fire predictions, they are only limited to surface fire spread rates in forests and rangelands. Also, fire predictions, spread rates and intensity in live vegetation from these models are not very accurate (Engstrom et al., 2010).

In order to predict fire transition from surface to the tree crowns and for predicting flare-ups, integration of combustion data for live vegetation must be carried out to improve current forest fire models. This integration makes the current CFD models too

cumbersome to solve with direct calculation method and it is also very computationally expensive and may take months to complete. On the other hand, the empirical models are too simple and there is not enough empirical data that describe fire transition from surface to the tree crowns and flare-ups.

The advancement in the field of computer science, engineering and computer technology has made computer modeling one of the fastest growing fields in fire protection engineering. The current trend of computer technology and capability make CFD modeling of fires very attractive. For instance, the long computational time required to solving a heat transfer problem in three different modes - conduction, convection and radiation in the fire engineering by using relatively small grid size has been greatly reduced with the help of computer modelling or numerical simulations; unlike several hours, days and even months that were dedicated to solving the same problem in previous years. Also, as computer simulations errors are easily detected and corrected; the results are easily traceable as well. Computer technology offers many advantages as compared to experimental approach. Compared to the experimental cost, computer simulations are affordable. The result of the simulation can be compared with the laboratory experiment. The comparison by Wren et al. (2006) showed that CFD is still the most accurate as shown in figure 1.0 but the slowest. Upon validation, if results from model and experiment are similar with only minimal deviations, the model can be considered for fire predictions.

The National Institute of Standards and Technology (NIST) developed and released a computational fluid dynamics model known as Fire Dynamics Simulator (FDS) in February 2000. It is considered the best tool in the history of fire behavior modeling.

Although, there were certain restrictions in the earlier versions of the software, the latest version of FDS has a lot of improvement in an attempt to resolve all restrictions and comments from the researchers and end users. As of today, NIST released the sixth version of FDS in April, 2013.

According to FDS application user manual (McGrattan et al., 2013), FDS can be defined as a CFD model of fire driven fluid flow. It makes use of numerical simulation to solve the Navier-Stokes equations appropriately for low-speed, thermally-driven flow with an emphasis on smoke and heat transport from fires. NIST developed Smokeview as a plotting and visualization tool to display results from FDS.

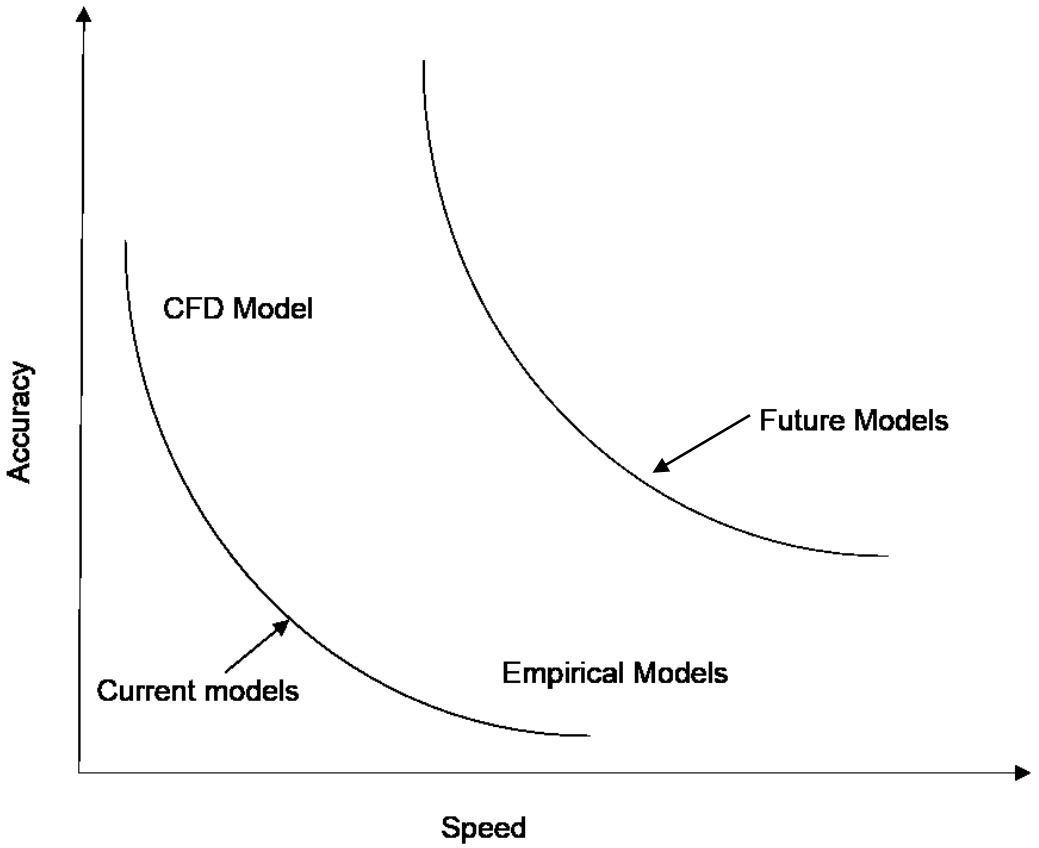

Figure 1. Comparison of different fire models

Section 2 of the thesis describes the Physics of the FDS. FDS deployment is described in Section 3. Experimental setup in explained and Section 4 followed by experimental results in Section 5 and FDS results in Section6. Conclusions are summarized in Section 7.

2.0 Physics of Fire Dynamic Simulator

2.1 Numerical Grids

FDS is a computational fluid dynamics (CFD) model which solves numerically a discretized form of the Navier-Stokes equations for low speed, thermally-driven flow and/or scalar transport in fire structures (NIST, 2013). Each of the computational element or control volume is a zone which can be as large as meters on each side or small as millimeters. The smaller the grid size, the more accurate the model, but the computational cost grows. Since the computational domain usually consists of a volume within the entire compartment, rectilinear grids are the most obvious and simplest numerical grids applicable. And because FDS is a large eddy simulation (LES) model, uniform meshing is preferred (Figure 2), or mesh can be stretched in one or two of the three coordinate directions. Once the mesh is established, it is very easy to define rectangular obstructions that define the geometry based on the resolution determined by the grid.

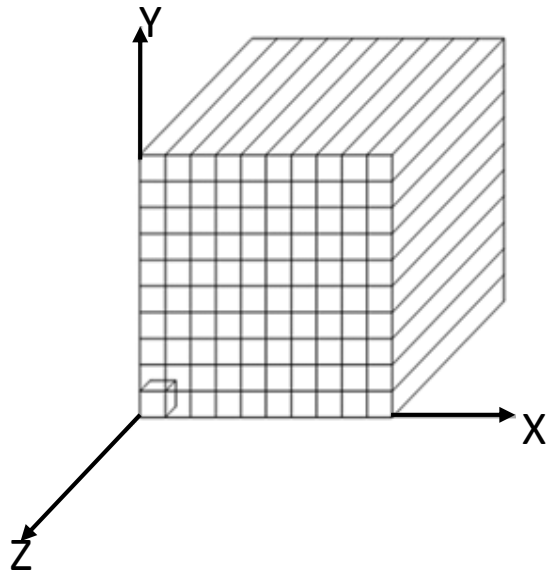

Figure 2. Three dimensional grids

2.2 Fluid Mechanics in FDS

The governing equations are approximated using second-order accurate finite differences on a collection of uniformly spaced three-dimensional grids (McGrattan et al., 2013). FDS uses finite difference method (FDM) to solve partial derivatives of the conservation equations of mass, momentum and energy and the solution is updated in time on a 3-D rectilinear grid. Since there exists no analytical solution for the fully-turbulent Navier-Stokes equation, numerical methods becomes the right solution where the compartment is divided into a three-dimensional grid or small cubes known as grid cells (Figure 2). The model calculates the physical conditions in each cell as a function of time. The basic set of the conservation equations for mass, momentum and energy which is solved by FDS is shown below.

2.2.1 Conservation of Mass

The mass conservation for incompressible flow is given by

$$\frac{\partial \rho}{\partial t} + \nabla \cdot \rho \vec{u} = 0 \qquad (1)$$

where, $\vec{u}$ is velocity vector whose components are *u, v* and *w,* in *x, y,* and *z* respectively, ρ is fluid density and *t* is time. Practically, the conservation of mass can be described as (if the density, ρ is constant): what flows in to a control volume must flow out. The conservation of mass states that the rate of mass storage, due to density changes within a control volume is balanced by the net rate of inflow of mass by convection (Smardz, 2006).

2.2.2 Conservation of Momentum

The conservation of momentum, Newton's second law of motion, states that the rate of change of momentum of a fluid element is equal to the sum of the forces acting on it (Cox, 1995):

$$\rho\left(\frac{\partial \vec{u}}{\partial t} + (\vec{u}\cdot\nabla)\vec{u}\right) = -\nabla p + \rho\vec{g} + \nabla\cdot\tau\,. \qquad (2)$$

The left hand side of this equation expresses the rate of change of momentum of a volume of fluid, the right hand side reflects the forces acting on it. The forces usually include gravity (g) a body force, pressure (p) and shear stresses (τ) as surface forces acting on the fluid within the control volume. Gravity is important as it represents the influence of buoyancy on the flow. The viscous stress is given by the product of viscosity and gradients of velocities that the fluid volume is subjected to. For Large Eddy Simulations, Smagorinsky model is used to account for the sub grid effects (McGrattan et al., 2002). This uses the deformation factor to arrive at a value for the local turbulent viscosity based on the fluid density, an empirical constant and a characteristic length which is in the order of the grid size used in the model. The turbulent viscosity is then used to calculate thermal conductivity and diffusivity for the model (Smardz, 2006).

2.2.3 Conservation of Energy

The energy equation accounts for the energy accumulation due to internal heat and kinetic energy, as well as the energy fluxes associated with convection, conduction, radiation, the inter diffusion of species and the work done on the gases by viscous stresses and body forces. In general it describes the balance of energy within the control volume.

The FDS model uses the following form of the energy balance equation:

$$\frac{\partial}{\partial t}(\rho h) + \nabla \cdot \rho h \vec{u} - \frac{\partial \rho}{\partial t} + \vec{u}\nabla\rho = q''' - \nabla \cdot q_r + \nabla \cdot k\nabla T + \nabla \cdot \sum_i h_i \, (\rho D)_i \nabla Y_i. \quad (3)$$

where $h = \sum_i h_i \, Y_i$, h_i is the convective heat transfer coefficient, k represents the thermal conductivity, Y_i is mass fraction of species i, q_r is radiative heat transfer, T is temperature and D is the diffusion coefficient.

2.2.4 Equation of State for a Perfect Gas

Equation of state at standard temperature and pressure is represented by:

$$P = \rho \frac{RT}{M} \quad (4)$$

where P is the pressure, R is the gas constant, and M is the molecular weight of the fuel.

2.2.5 Conservation of Species

The mass conservation equation in terms of mass fractions of the individual gaseous species can be presented as conservation of species equation:

$$\frac{\partial}{\partial t}(\rho Y_i) + \nabla \cdot \rho Y_i u = \nabla \cdot \rho D_i \nabla Y_i + \dot{m}_i''' \quad (5)$$

1st term 2nd term 3rd term 4th term

The first term is the accumulation of species due to a change in density. The second term represents the inflow and outflow of species. The third term gives the inflow or outflow of species from the control volume due to diffusion while, the fourth term describes the production rate of the particular species.

2.3 Combustion Model in FDS

The chemistry of fire is a reaction between hydrocarbon fuel and oxygen that produces carbondioxide and water vapor. This definition is an ideal description of combustion process when air is considered 100% oxygen. However, fire is a relatively inefficient combustion process involving multiple fuel gases that contain more than just carbon and hydrogen atoms as shown in the equations below.

$$\alpha(C_lH_mO_z)_n(g) + \beta O_2(g) + \gamma N_2(g) \rightarrow bCO_2(g) + \gamma N_2(g) + jH_2O(g) + \lambda C_lH_m + \text{Heat} \quad (6)$$

$$C_{(s)} + O_{2(g)} \rightarrow CO_{2(g)} + \text{Heat} \quad (7)$$

$$CO_{(g)} + 0.5O_{2(g)} \rightarrow CO_{2(g)} + \text{Heat} \quad (8)$$

$$2H_{2(g)} + O_{2(g)} \rightarrow 2H_2O_{(g)} + \text{Heat} \quad (9)$$

$$CH_{4(g)} + 2O_{2(g)} \rightarrow CO_{2(g)} + 2H_2O_{(g)} + \text{Heat} \quad (10)$$

where *α, β, γ, λ, b, j* are stoichiometric ratios of the reactants and the products and *l, m, n* are number of atoms in each molecule.

The equation (6) above showed that the number of gas species to keep track of in the simulation is almost limitless.

For that reason, in order to make the simulations tractable, the following assumptions are made:

1. The number of fuels is limited to one.
2. The number of reactions is just one or, at most, two.
3. The incoming air stream is left open because there is a possibility that the reaction may not proceed due to the lack of sufficient oxygen.
4. The air is neither fuel nor products but treated as a single gas species (lumped species).

FDS makes use of the mixture fraction model as the default combustion model to run the simulations. It is simply defined as the fraction of gas at a given point in the flow field that originated as fuel, and it is considered a conserved scalar quantity.

The model assumption is that combustion is mixing-controlled, and that the reaction of fuel and oxygen is infinitely fast. The mass fractions of all of the major reactants and products can be derived from the mixture fraction by means of "state relations," empirical expressions arrived at by a combination of simplified analysis and measurement (Smardz, 2006).

$$Z = \frac{sY_F - (Y_O - Y_O^{\infty})}{sY_F^I - Y_O^{\infty}} \; ; \; s = \frac{\nu_O M_O}{\nu_F M_F} \tag{11}$$

The variable *(Z)* is the mixture fraction which represents the mixing controls combustion and species of interest. $Y_{F,\ and}\ Y_0$ are the mass fractions of the fuel and oxidizer in the mixture. sY^I_F represents the fuel mass fraction in the pure fuel stream. sY_0^{∞} denotes the oxidizer mass fraction in the oxidizer stream. *S* gives is called the stoichiometric mass ratio. ν_0 and ν_F are the stoichio-metric coefficients of the oxidizer and fuel. M_0 and M_F are the molecular weights of oxidizer and fuel respectively.

The above equation is a simple combustion model where mixture fraction varies from Z =1 in a region containing only fuel to Z =0 in regions far away from the fire where the ambient air rich in oxygen is present.

It is interesting to note that the combustion model approximates the combustion process in both space and time so as to simulate the fire more efficiently (Floyd et al., 2013).

Another assumption in combustion model is that large scale convection and radiative transport can be modeled directly while small scale mixing can be ignored. Since the combustion processes are on a much shorter time scale than what is obtainable in the convection processes, an infinite reaction rate is assumed (Spearpoint, 2004). The fuel and oxygen cannot co-exist (McGrattan et al., 2002). Subsequently, a point is reached where both species instantaneously disappear, their mass fractions diminishing to zero. This leads to a more simplified equation as shown below to determine the flame mixture fraction (Z_F).

$$Z_F = \frac{Y_O^\infty}{sY_F^{Ii} + Y_O^\infty} \tag{12}$$

The point Z_F which defines the flame in the computational domain (Floyd et al., 2001) is referred to as the flame sheet. The basic assumption that fuel and oxidizer cannot co-exist leads to the 'state relation' between the oxygen mass fraction Y_0 and Z_F (McGrattan et al., 2013).

$$Y_o(Z) = Y_o^\infty \left(Z - \frac{Z}{Z_f}\right) \quad Z<Z_F \tag{13a}$$

$$0 \qquad Z>Z_F$$

For a stoichiometric mixture, fuel and oxygen are completely consumed at the end of combustion.

$$Y_F = Y_o = 0 \tag{13b}$$

However, if $(Z < Z_F)$ fuel is deficient and the mixture is called fuel lean, then, combustion terminates when all the fuel is consumed $(Y_F = 0)$. Similarly, if $(Z > Z_F)$ oxygen is deficient and

the mixture is called fuel rich ($Y_0 = 0$). Combustion then terminates when all the oxygen is consumed.

The mass fraction of all other species of interest can be described by individual state relations based on the mixture fraction. This detail explanation is in Floyd et al. (2013).

The oxygen consumption rate (m_o''') can be determined using the local oxygen mass fraction. This is then used to calculate the local HRR by multiplying it with the HRR per unit mass of oxygen (ΔHo) (McGrattan et al., 2013).

The mixture fraction model has several limitations, both numerical and physical. The numerical limitations are related to the resolution of the underlying numerical grid (Spearpoint, 2004).

One problem that occurs due to the local HRR calculation procedure is that the flame surface defined by the mixture fraction $Z = Z_F$ will tend to underestimate the observed flame height if the fire is not adequately resolved.

For fire scenarios the relationship between the fire's characteristic diameter, D*, and the size of the grid cells, δx, will indicate the accuracy of LES modeling of the sub-grid motion of fluids. The characteristic diameter is calculated from:

$$D^* = \left(\frac{\dot{Q}}{\rho C_p T\sqrt{g}}\right)^{\frac{2}{5}} \quad (14)$$

where, $\dot{Q}$ is the heat release rate of the fire in kW, and C_p is the specific heat. A more accurate estimate of the flame height can be determined by using a different value for the mixture fraction (*Z*). Higher values of $D^*/\delta x$ means that a larger part of the fire dynamics is solved directly.

The effective mixture fraction ($Z_{f,eff}$) is given by:

$$\frac{Z_{F,eff}}{Z_F} = min\left(C\frac{D^*}{\delta x}\right) \quad (15)$$

where, *C* is the empirical constant (McGrattan et al., 2002).

2.4 Thermal Radiation Model in FDS

FDS uses a modified finite volume method to calculate the radiative fluxes during simulations. The method is derived from the Radiative Transport Equation (RTE) for non-scattering grey gas (Hume, 2003). This method relates radiation intensity to wavelength. What the FDS does is assigning the temperature generated from the flame sheet to the adjacent cells, this lowers the temperatures since the temperature in the cell is averaged compared to a point in the diffusion flame. And since radiation is dependent on the fourth

power of temperature, this method of assigning temperature can have a significant impact on the calculated radiation. In this way the temperature elsewhere is calculated with best possible confidence so that the source term can assume its ideal value (McGrattan et al., 2002). The equations below describe radiation relations:

$$\kappa I_b = \kappa\sigma T^4/\pi \quad \text{Outside flame zone} \qquad q''' = 0 \tag{16}$$

$$\kappa I_b = C_\circ \kappa\sigma T^4/\pi \quad \text{Inside flame zone,} \qquad q''' > 0 \quad \text{or} \tag{17}$$

$$\kappa I_b = \chi_r q'''/4\pi \quad \text{Inside flame zone}$$

where, $C_\circ$ is constant computed at each time step. χ_r is the local fraction of the heat release rate emitted as thermal radiation. q''' is the heat release rate per unit volume. κ is the local absorption coefficient which is dependent on the mixture fraction and temperature. T is the temperature of the flame. Finally, I_b is the intensity of radiation, and σ is the Stefan-Boltzman constant (McGrattan et al., 2013).

3.0 FDS Deployment

This section of the thesis gives a brief account of the scientific and mathematical principles used by FDS. It is not the intention of this section to discuss the model in great detail. There are several pieces of work that discuss the fundamentals of the model, such as FDS technical guide (McGrattan et al., 2013), research projects by Petterson (2002), and Hume (2003).

3.1 FDS Model Setup

FDS is a free software package that can be acquired online at http://www.fire.nist.gov/fds/.

The user builds an input file which contains detail information such as grid size, ambient environment, geometry of the scenario being modelled, boundary conditions, material properties, the fire itself, and required outputs. The simulation from FDS generates output files based on the contents in the input file. The output of the simulation can be displayed on an animated complimentary program known as Smokeview built into the FDS software. The flow chart in (Figure 3) shows the components of FDS setup.

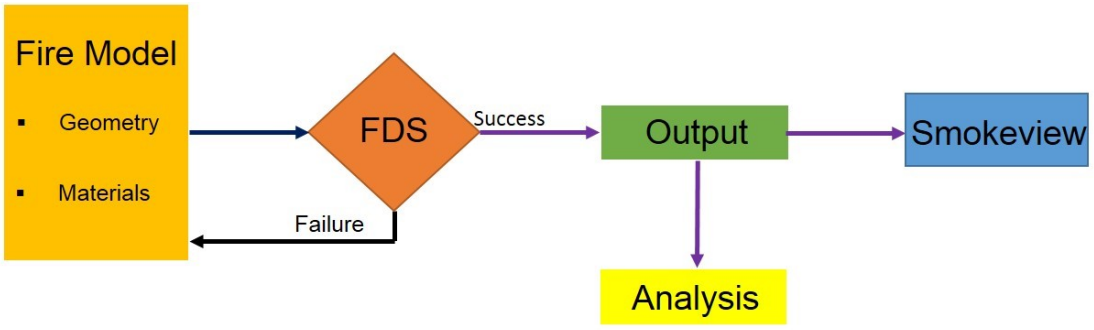

Figure 3. Components of FDS model setup

3.1.1 Procedure

FDS runs on a fairly simple command prompt as long as the location of the input file is known. Since the simulation generate so many output files, it is recommended to make a folder for each input file.

To run the FDS model the following steps are required.

1. Go to Run from the Start menu, then type cmd and press Enter key,
2. In the command prompt type cd and press Enter key,
3. Type directory then press Enter key,
4. Type the name of the sub-directory where the input file is saved and press Enter key,
5. Type fds, and the input file name.txt, then press Enter key.

The simulation will start immediately and run successfully if there are no errors. In order to view the output of the simulation, open the folder created earlier and double click on the Smokeview exe file. An animated picture is displayed on the computer screen to analyze the results. The FDS input file that generated the 2D Smokeview image in Figure 4 is in Appendix A.

3.1.2 Output from Smokeview

To visualize the model output we use the Smokeview package in FDS. Smokeview is a program designed to visualize numerical calculations generated by the FDS. Smokeview uses quantitative display techniques such as 2D and 3D contouring. The realistic display of data means presenting the data in a form as it would actually appear in real life (Glenn, 2013).

Figures 4 through 7 are taken from Smokeview visualization in different stages of fire. In Figure 4, at the very beginning of fire, we cannot see any flames despite the slight temperature increase. Little or no change is observed in the physical state of the fuels at 0.9 seconds after ignition.

At 1.92 seconds into the simulation (Figure 5) the fuel has reached its ignition temperature and a flame is developing. Figure 6 presents flame propagation through both, surface and crown fuels. This takes place rapidly until all fuel is consumed. The burnout stage where both surface and crown fuels are completely consumed is given in Figure 7. A sharp drop in temperature takes place at this stage. More Smokeview results for different layouts are displayed in Appendix A.

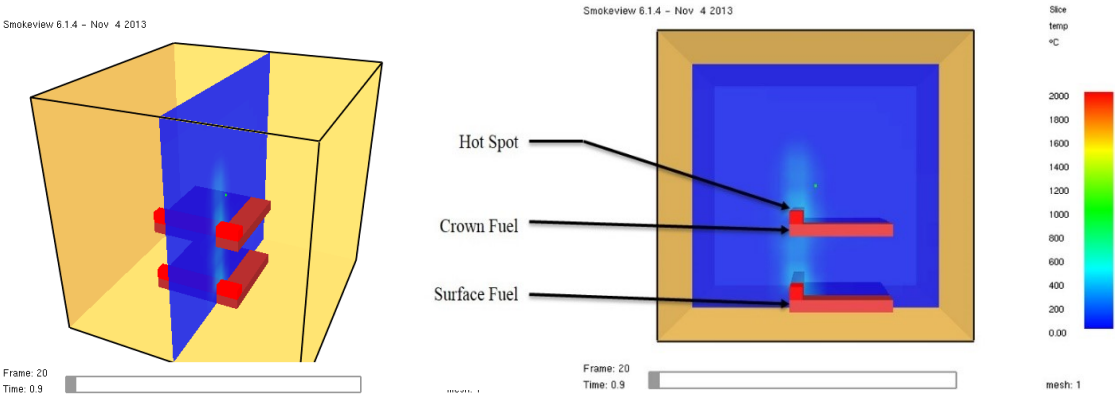

Figure 4. 2D & 3D Geometry of output before burning.

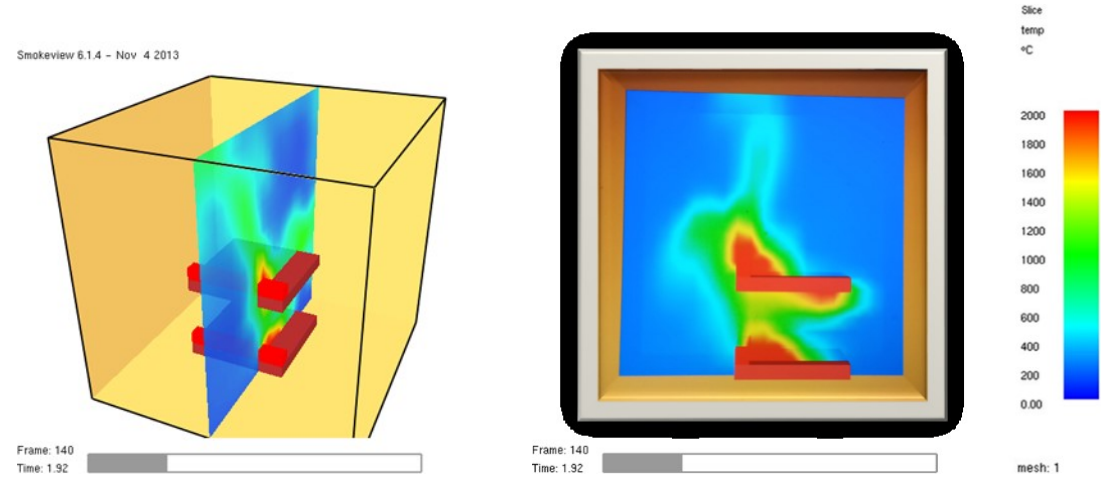

Figure 5. Geometry of output at the beginning of burning.

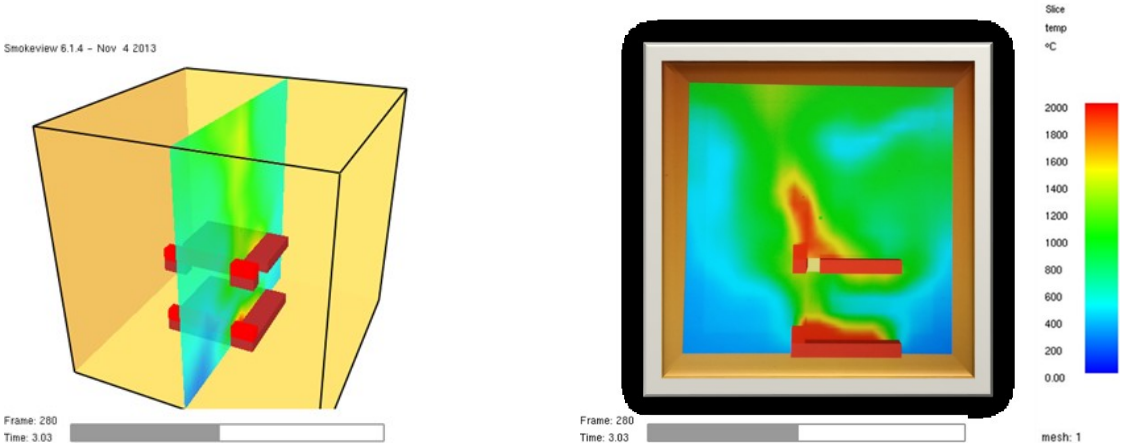

Figure 6. Geometry of output at the beginning of charring.

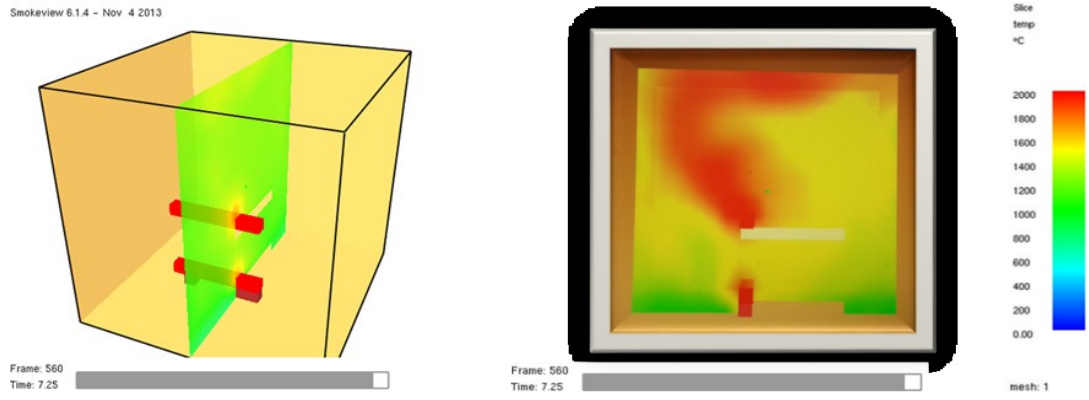

Figure 7. Geometry of output when burning is completed.

4.0 Experimental Setup

The laboratory-scale experimental setup conducted at the (USDAFS, PSW) research station, Riverside, California was carried out using the following procedures. In order to ensure accuracy of the experimental data, the experiment was repeated several times. This reduces uncertainties in the obtained experimental data, and model predictions may be more confidently compared to experimental results.

4.1 Procedure

Procedures for the experimental setup are highlighted in the following sections. Sketches and pictures are used to better understand the processes involved.

4.1.1 The Equipment Setup

The wind tunnel that we deployed for the laboratory experiments is made up of two sections. First, there is the fan section that is operated at a frequency of 40Hz to deliver the required wind speed of 1.0 meter per second. The second compartment is the test section which consists of the surface fuel bed that is made of fire proof insulator, and ten thermocouples that are equally spaced to measure flame temperature and flame speed. This section also contains the crown fuel bed made from a coarse wire mesh with 2.54 cm hexagonal size suspended on four load cells that measure the mass loss rate during the burning process. The wire diameter is 0.9 mm, and thus the percentage of open area is 85%. This ensured that the hot gas flow, originating from the surface fire, was relatively unobstructed except for the presence of the crown fuel. On this mesh, within the crown fuel, five thermocouples are arranged in the same manner as in the surface fuel bed. Figure

8 is a pictorial representation of the wind tunnel used for the fire behavior modeling experiment.

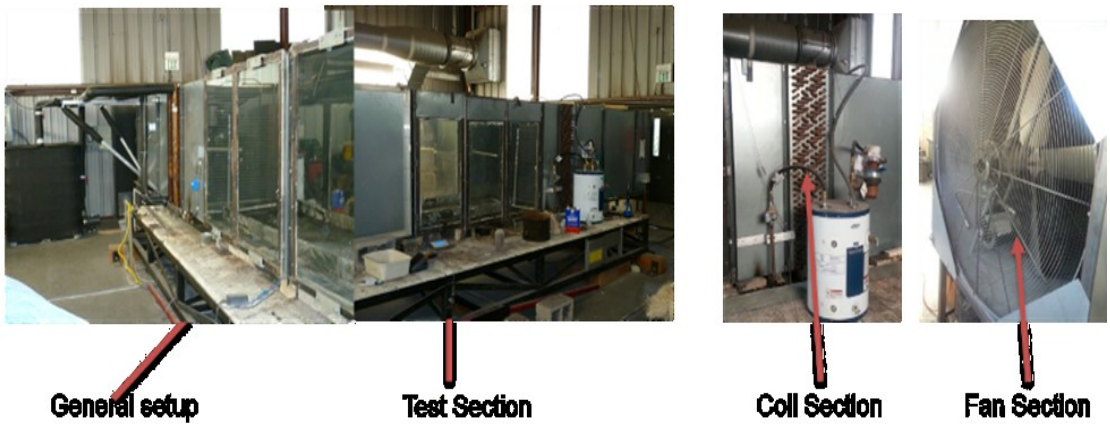

Figure 8. Experimental setup for fire transition from surface fuel to elevated crown fuel

4.1.2 Measurement and Loading of Fuels

The first step in loading of the two fuels was measuring the weight of excelsior and chamise on the calibrated scale positioned on the work table as shown in Figure 9 (a - f).

Figure 9. Diagrams showing the types of fuels and scales used during the experiment.

A mass of 0.50 Kg of aspen excelsior - Populus tremuloides, (Figure 9a) with fuel particle diameter of 1.0 mm, was weighed on a calibrated scale (Figure 9e) and later transferred to the surface fuel bed (Figure 10b). The fuel was evenly distributed over the entire 2.82m x 0.8m surface to a depth of 0.1 m. The calculated bulk density of aspen excelsior was 3.0 $Kg.m^{-3}$.

2.0 Kg of live chamise - Adenostoma fasciculatum (Figure 9b) with foliage diameter of approximately 5mm and branch diameter of approximately 3.5mm was also weighed and spread evenly over the crown fuel bed 1.82m x 0.62m to a depth of 0.2m (Figure 10c) top upper region. All chamise are about the same size and were collected from the same field location in Riverside County, California. The mass proportions of foliage and branch were 53% and 47%, respectively while the bulk density based on the volume occupied by fuel was 9.2 $Kg.m^{-3}$. Both bulk densities were held constant throughout all experiments. Figure 10 represents the loading of fuels at the wind tunnel.

(a) (b)

Figure 10. (a) diagram showing the position of the thermocouples during loading, (b) loading of both surface and crown fuels.

Figure 10. (c) Diagram showing a completely loaded fuel beds ready for ignition.

The work compiled by Susott (1982) described the physical properties of excelsior as follows: fuel particle density is 400 $kg.m^{-3}$, surface-to-volume ratio is 4,000m^{-1}, moisture content is 18%, heat of char combustion is 32.37 $MJ.kg^{-1}$, char content is 15.40%, and ash content is 0.35%. Similarly, the live chamise foliage leaves contain 500 $kg.m^{-3}$, 8,000m^{-1}, 84%, 31.35 $MJ.kg^{-1}$, 28.60%, and 3.50%, respectively, for the fuel particle density, surface-to- volume ratio, moisture content, heat of char combustion, char content, and ash content (Ragland et al., 1991) and Susott, (1982) compiled the live chamise properties as 600 kgm^{-3}, 1,143m^{-1}, 84%, 31.35 $MJkg^{-1}$, 14.30%, and 0.50%, respectively (Tachajapong et al., 2009).

4.2 Surface Fuel Ignition

The surface fuel was ignited along a line parallel to its width of 0.8 m. To ensure rapid ignition, approximately 2ml of ethyl alcohol were sprayed uniformly over this width. Ignition was accomplished at the center of the line with a hand-held igniter, and a line fire was established in less than a second. An important property of the crown fuel matrix is crown fuel bulk density. Higher crown fuel bulk density may increase the possibility of crown fire initiation by increasing the thermal energy accumulated within the crown fuel matrix and reducing convective energy loss to the surroundings (Tachajapong et al., 2008).

5.0 Laboratory Results and Discussions

This section discusses the results of the experimental observations and theory in great detail. The first section presents observations, followed by the analysis of the experiments.

5.1 Observations

This section gives a qualitative account of experimental observations. These include:

- Fire growth variations
- Relationship between the flame height and intensity
- Smoke layer development
- Increase of radiation with increased fire. This was felt through the observation window.

The effect of varying crown height and wind speed on flame propagation was investigated experimentally as described before. Figure 11(a) represents the surface fire under no wind condition (0 ms^{-1}), while in figure 11(b), surface fire spread was investigated 1.0 ms^{-1} wind (40 Hz fan setting).

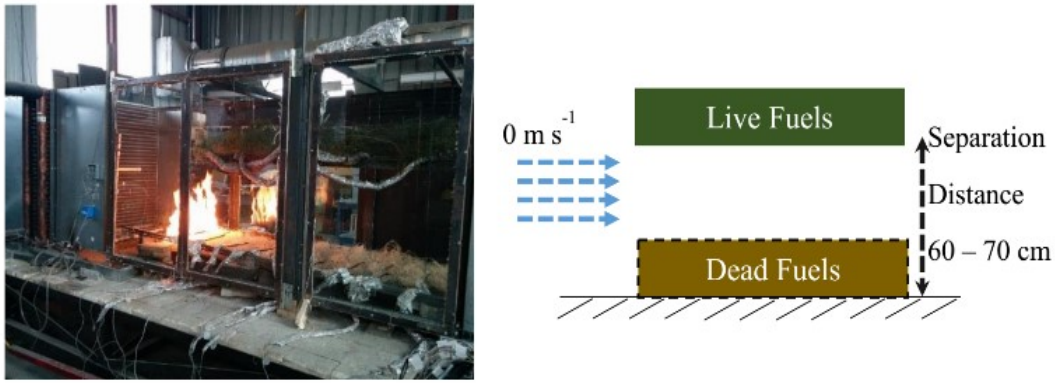

Figure 11 (a) Flame spread under no wind condition

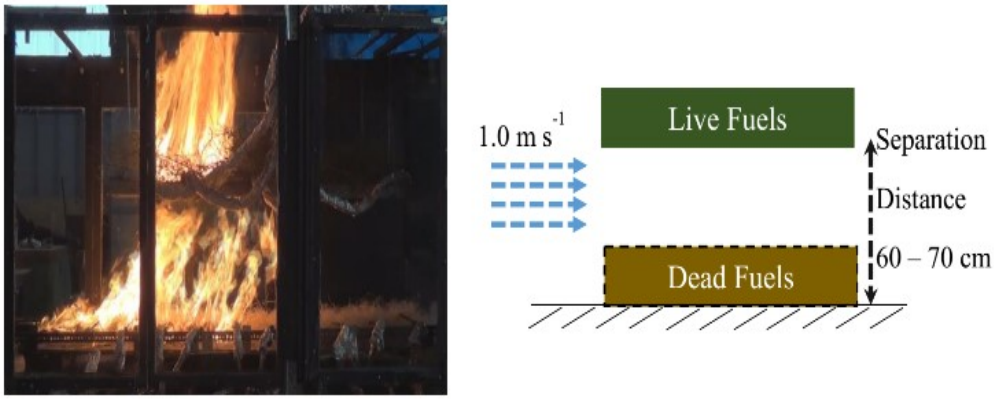

Figure 11 (b) Flame spread under 1.0ms^{-1} wind condition

5.1.1 Measuring Wind Speed

In order to validate the effectiveness of wind application during the experiment, the centerline velocity profile was measured used 40Hz fan setting. Readings were taken within loaded fuel test section. Three points were selected: 8cm above the surface fuels, 30cm between fuel beds, and above the crown fuels, 79cm from the base level. One minute

wind speed averages were taken with an Omega hot wire anemometer. Under free wind flow (unobstructed) condition, the measured speed was 1 m s^{-1}. However, half the speed (0.5 m s^{-1}) was recorded when the wind tunnel was loaded with surface and crown fuel. This observation shows that presence of fuels in the test section (surface and crown) influenced the flow within the test section as shown in Figure 11 (c).

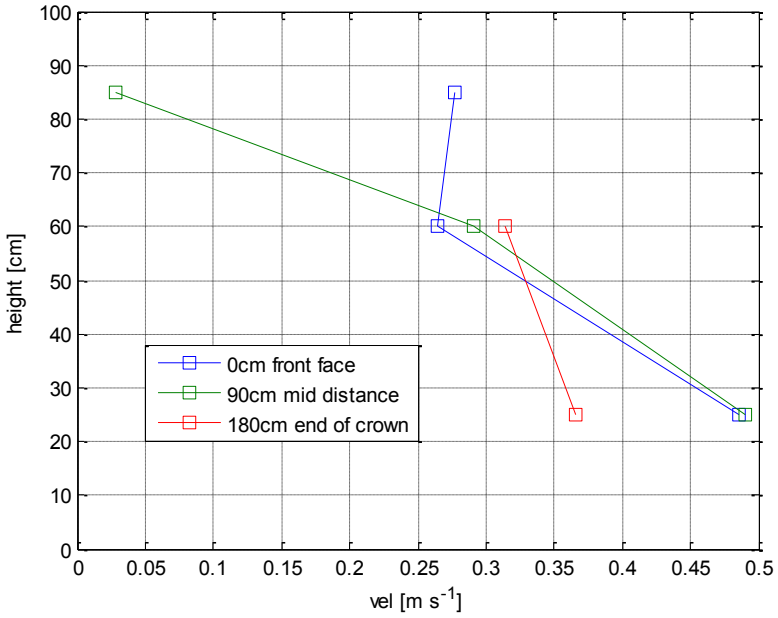

Figure 11 (c) Wind speed measurements in the wind tunnel.

5.1.2 Classification of Experiments

The experiments were classified under six subgroups for thorough analysis and presentation of the results. The letters A, B, C, D, E, and F represent the experiment class based on the controlled variables as summarized in Table 1. Figure 12 shows the continuous and intermittent region of the flame.

Table 1: Classification of Experiments based on controlled variables

Classification	Surface Fuel Bed	Wind	Observed Flame Region
A	-	-	-
B	-	X	-
C	X	-	Continuous
D	X	-	Intermittent
E	X	X	Continuous
F	X	X	Intermittent & Continuous

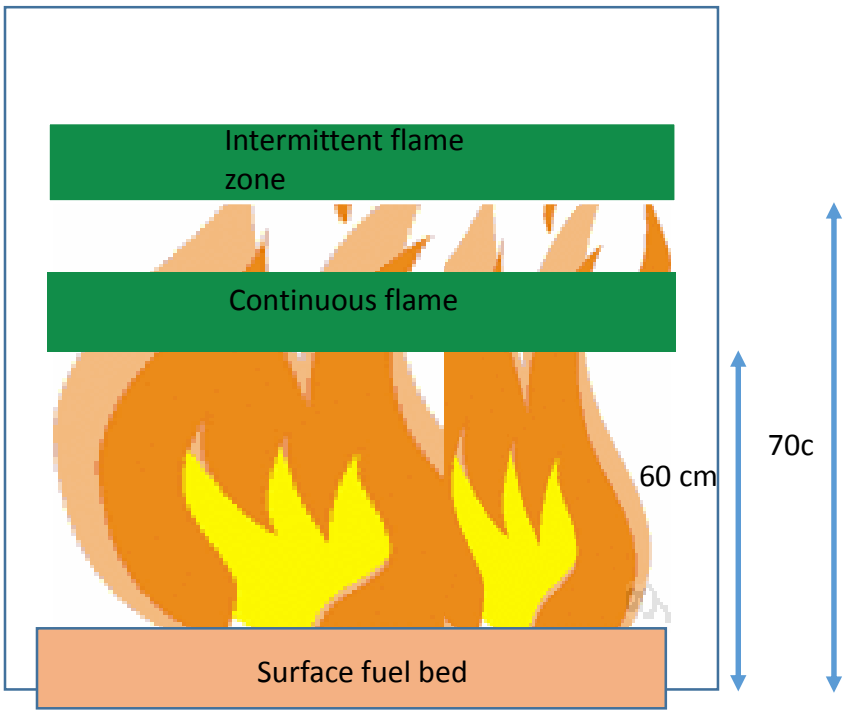

Figure 12. Continuous and intermittent regions of flame

The interaction between crown and surface fuels was investigated for different fuel bed separation distance, wind speeds, fuel moisture content and presence of surface fuel bed. The experiments were repeated at least 9 times and the fuel moisture contents were taken for each experiment. Table 2, summarizes the parameters of each experiment. These include the date, experiment number, mass of surface fuel, mass of crown fuel, crown fuel moisture content, ambient temperature, ambient humidity, and fan speed setting.

The thermocouple data in Figure 13 shows that the hot gas that originated from surface fire supplied convective heating to the crown fuel and raised its temperature to 564 K above the ignition temperature of Chamise (which is 523K, Babrauskas, 2002). Ignition temperature is the critical fuel temperature at which flaming combustion is initiated (Saito, 2001; Williams, 1982).

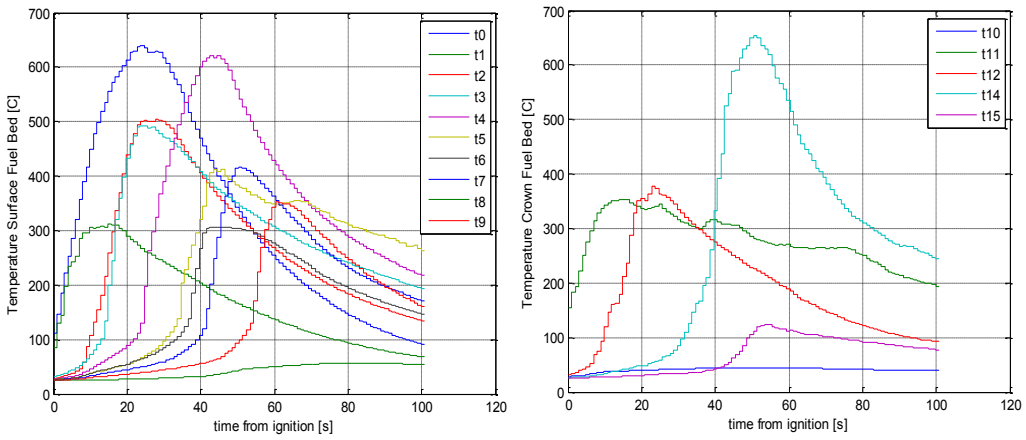

Figure 13. Thermocouple data for experiment 22

Other earlier works suggested a range of ignition temperature for live foliage samples between 500–600K (Babrauskas, 2002; Engstrom et al., 2004), but the most commonly reported ignition temperature for Chamise is 523 K. A small part of the crown fuel ignited first and burned in smoldering mode and then transitioned to flaming combustion.

Table 2: Summary of experiment parameters.

Exp	Crown Mass [g]	Fuel Bed Mass [g]	Fan Speed [Hz]	Crown Height [cm]	Case Type	Ambient Temperature [F]	Relative Humidity [%]	Fuel Moisture Content [%]
1	2500	500	0	70	D			
2	1000	500	40	70	F			
3	1000	500	0	70	D			
4	1000	0	0	70	A	72	39	
5	1000	0	40	70	B	72	39	
6	1000	500	0	60	B	72	42	
7	1000	500	40	60	E	72	42	
8	1000	500	0	60	C	71	49	7.06
9	1000	500	40	60	E	71	49	2
10	1000	500	40	60	E	71	49	7.06
11	1000	0	40	60	B	71	49	4.135
12	2000	0	40	60	B	71	49	4.135
13	2000	500	40	60	E	67	46	14.85
14	2000	500	0	60	C	67	46	14.85
15	2000	0	0	60	A	67	46	18.94
16	2000	0	40	60	B	67	46	14.85
17	2000	500	40	60	E	70	47.6	43.58
18	2000	500	0	60	C	70	47.6	43.58
19	2000	0	40	60	B	70	47.6	32.78
20	1000	500	40	70	F	70	47.6	43.58
21	2000	500	40	70	F	79	18	14.85
22	2000	500	40	70	F	75	25	14.85
23	2000	500	40	70	F	75	22	14.85
24	2000	500	0	70	D	74	40	14.85
25	2000	500	0	70	D	74	40	14.85
26	2000	500	0	70	D	74	40	14.85
27	2000	0	40	70	B	74	40	14.85
28	2000	500	40	70	F	78	17	65.92
29	2000	500	40	70	F	78	18	41.83

Exp	Crown Mass [g]	Fuel Bed Mass [g]	Fan Speed [Hz]	Crown Height [cm]	Case Type	Ambient Temperature [F]	Relative Humidity [%]	Fuel Moisture Content [%]
31	2000	500	40	70	F	78	18.6	65.92
32	2000	500	0	70	D	78	18.6	65.92
33	2000	500	0	70	D	81	20	23.88
34	2000	500	0	70	D	81	20	30.1
35	2000	0	40	70	B	81	20	30.1
36	2000	0	40	70	B	81	20	30.1
37	2000	0	40	71	B	81	20	30.1
38	2000	500	40	60	E	68	54	10.6
39	2000	500	40	60	E	68	54	10.6
40	2000	500	40	60	E	68	54	10.6
41	2000	500	40	60	E	71	65	80.7
42	2000	500	0	60	C	82	31	20
43	2000	500	0	60	C	82	26	20
44	2000	500	0	60	C	85	26	20
45	2000	500	0	60	C	88	16	20
46	2000	0	0	6E	A	88	16	20
47	2000	0	0	60	A	88	16	20
48	2000	0	0	60	A	88	16	20
49	2000	0	0	60	A	88	16	20
50	2000	500	0	60	A	89	16.5	12.1
51	2000	500	0	70	D	90	19.5	12.1
52	2000	500	0	70	D	90	19.5	
55	2000	500	40	60	E			
56	2500	500	40	60	E			
57	2000	500	0	60	C	83	18	26.18
58	2000	500	0	60	C	83	18	20.64
59	2000	500	40	60	E	83	18	20.64
60	2000	500	40	60	E	83	18	20.64
61	2000	500	0	70	D	89	11	
62	2000	500	40	70	F	82	31	18.56
63	2000	500	0	70	D	81	33	18.56
64	3000	600	40	70	F	83	38	18.56
65	2000	500	40	60	E			
66	2000	500	40	60	E	67	54	15.86
67	3000	600	40	60	E	67	58	15.86
68	2000	500	0	70	D	91	13	
69	2000	500	0	70	D	91	16	

Exp	Crown Mass [g]	Fuel Bed Mass [g]	Fan Speed [Hz]	Crown Height [cm]	Case Type	Ambient Temperature [F]	Relative Humidity [%]	Fuel Moisture Content [%]
70	3000	500	0	70	D	99	18	
71	0	2000	0	0	G	100	13	
72	0	2000	40	0	H	100	13	
73	0	2000	0	0	G	100	13	
74	0	2000	40	0	H	100	13	

Exp -Experiment

5.1.3 Flame Height

The flame height is a very important aspect of this study based on the fact that surface ignition of crown fuels greatly depend on flame height. Flame height for this study was calculated from video captures during the experiment. All the height observations presented in Figures 14 & 15 are the averages of minimum of five still images from the experiment video. A plot of flame height by each Experimental Classification is presented in Figure 14 and 15 for the surface fuels and class A and B. However, the crown flame height exceeded video frame and could not be calculated in categories C-F. Special experimental setup is needed to establish these flame heights. Since this was out of the scope of presented study such modifications are left for future work.

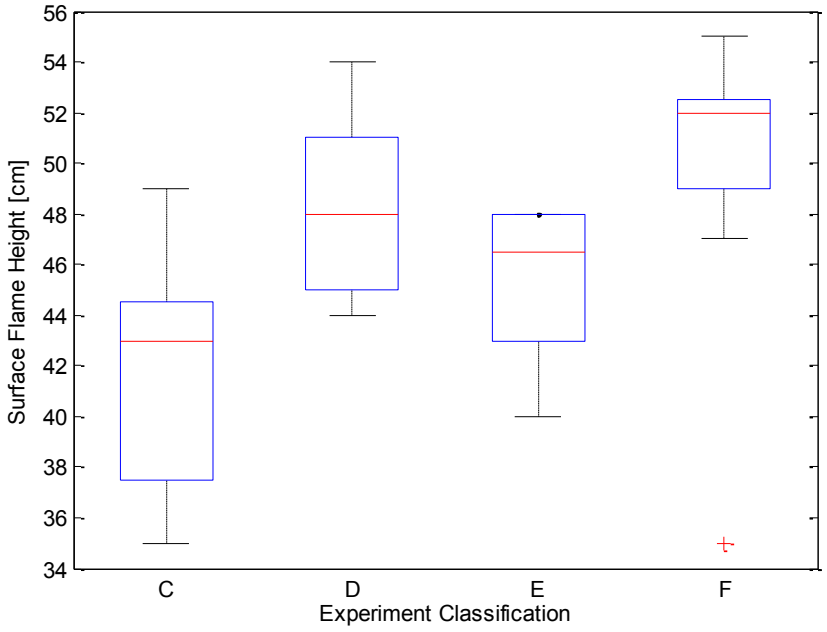

Figure 14. Surface flame height estimated from videos for each class.

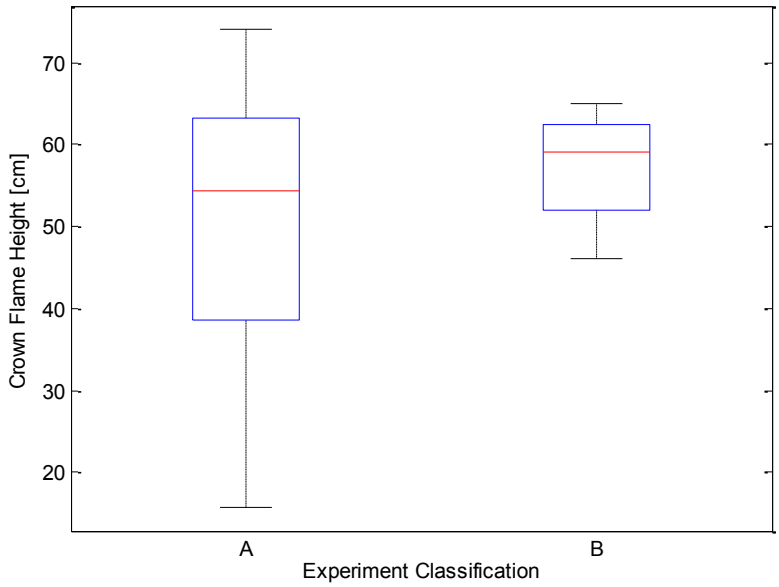

Figure 15. Crown flame height estimated from videos for classes A and B. Flame heights for other classes exceeded the recorded area.

Flame height and flame length are being used interchangeably in literature, but for the purpose of this research, the vertical component was referred to as flame height (Alexander and Cruz, 2012). Figure 16 taken from Alexander and Cruz (2012) illustrates the difference between flame length and flame height for both surface and crown flames.

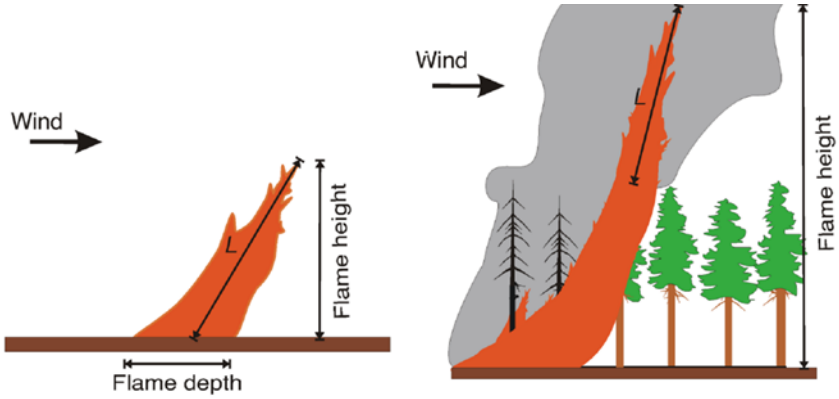

(a) (b)

Figure 16. Schematic diagram illustrating the distinction between flame length (*L*) and flame height in a (a) surface fire and (b) crown fire (copied from Alexander and Cruz 2012).

5.1.4 Flame Front Velocity Calculation

Flame propagation velocity was obtained from the analysis of thermocouple data after the experiment.

The thermocouples were equally spaced and spanned through the fuel bed. Figure 17 shows a typical thermocouple arrangement during the experiment.

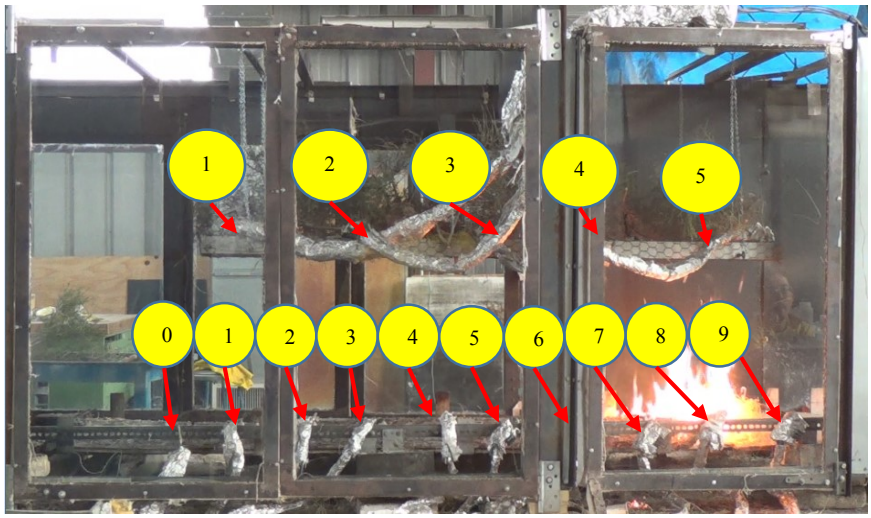

Figure 17. Horizontal positions of thermocouples in the fuel beds.
The thermocouples were embedded into the beds below the yellow circles.

The peak temperatures detected by thermocouples were used to calculate the flame propagation velocity by dividing the thermocouple distance with time between the temperature peaks. Averaging of the flame font velocities gives the flame front velocity for each experiment.

$$v_i = \frac{x_i - x_{i-1}}{t_i - t_{i-1}} \tag{18}$$

Where v_i is the flame front velocity at thermocouple i (i=1, 2….15), x is the position of thermocouple, and t is the time of the peak temperature for that thermocouple. Figures 17 show the fire experiment to measure the flame temperature using thermocouples.

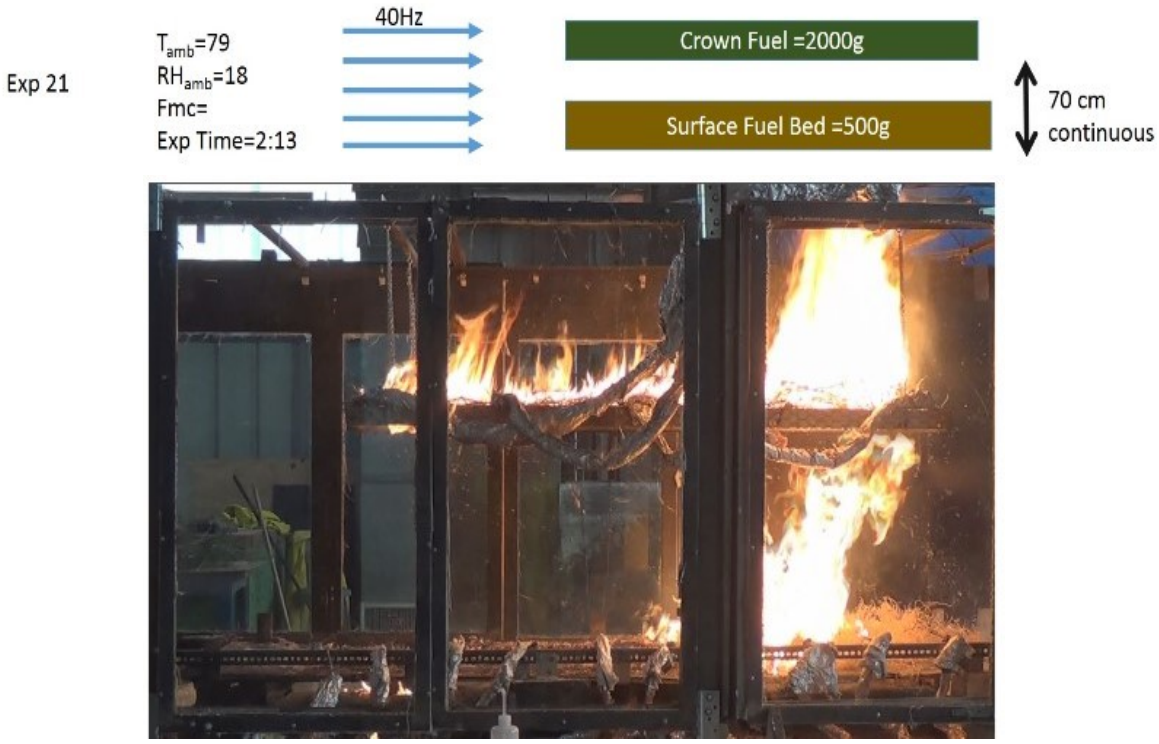

Figure 18. Temperature trace of the 10 thermocouples along the centerline of the surface fuel bed.

The thermocouple data of figure 18 is shown in figure 19 and 20. Looking at the graph, we see a rapid temperature increase as the flame front is approaching the thermocouple location followed by gradual cooling once the front passes that location.

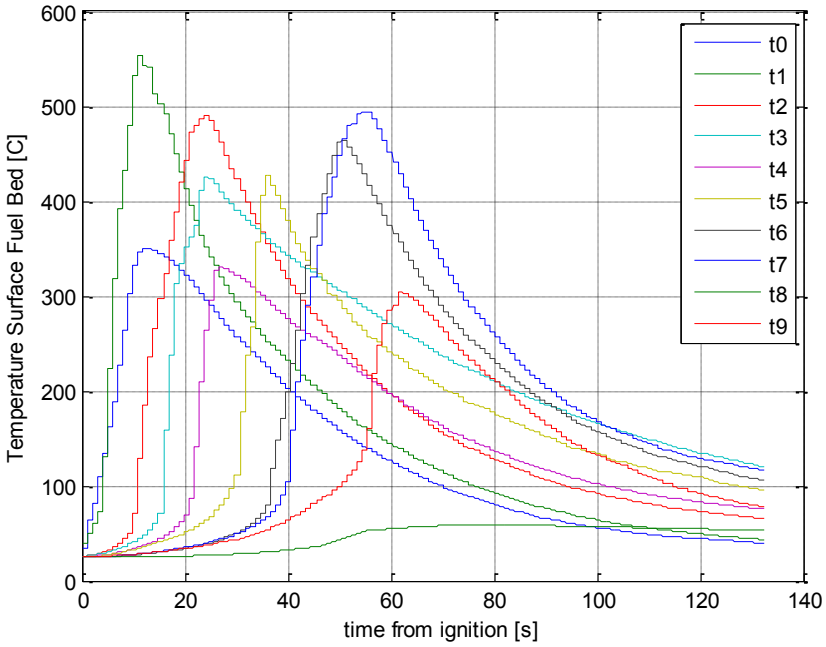

Figure 19. Temperature trace of the 10 thermocouples along the centerline of the surface fuel bed.

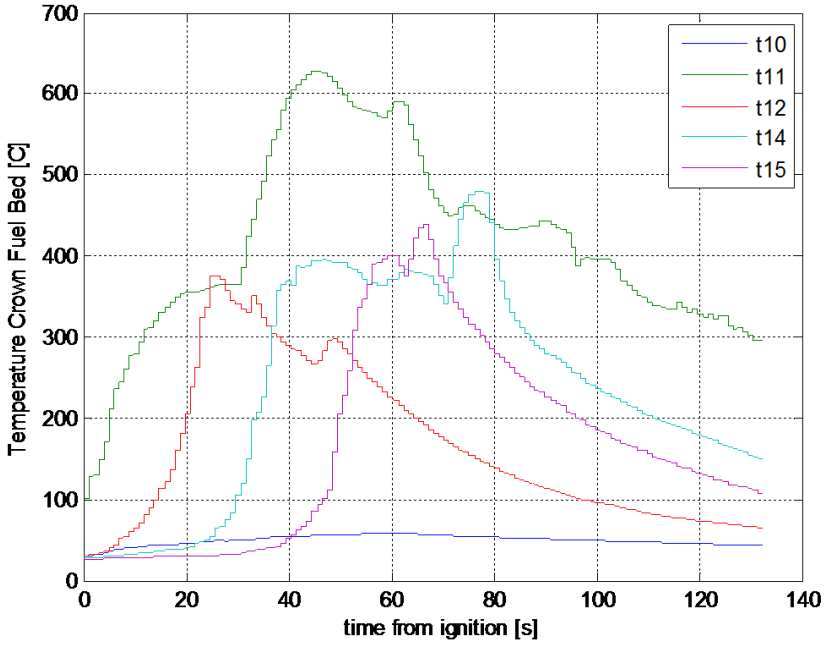

Figure 20. Temperature trace of the 5 thermocouples along the centerline of the crown fuel bed.

In order to analyze the flame front velocity, the video space was divided into sections. Propagation of the flame front was timed between entering and leaving sections. The flame front velocities for the surface fuels are presented in Figure 21. The presented values are averages through all the timed sections. It is important to report that in 4 of 8 experiments in class C and 2 of 8 experiments in class D, surface fuel failed to ignite the crown fuel. Similarly, cases such as experiments 4, 47, and 48 of class A where the crown exhibited passive flame characteristics like torching, but failed to spread were equally noted.

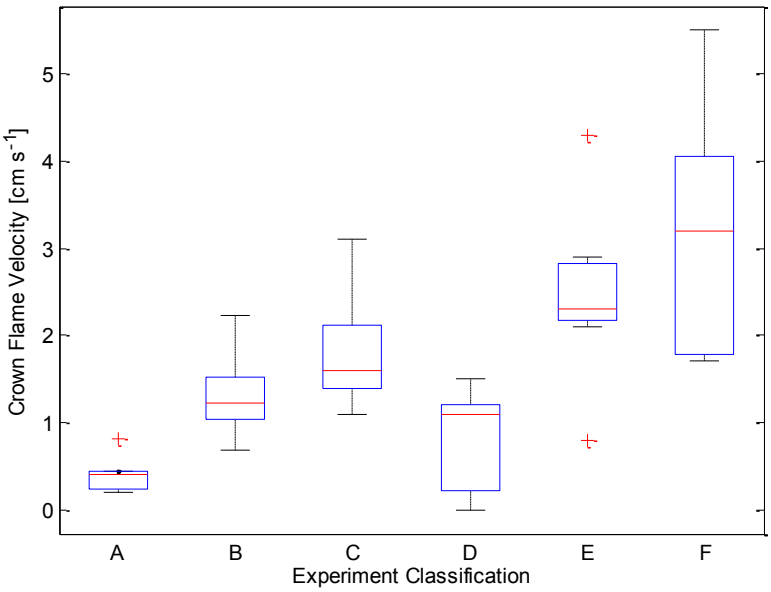

Figure 21 (a) Surface flame velocity by experiment classification. Flame velocity approximated from video analysis.

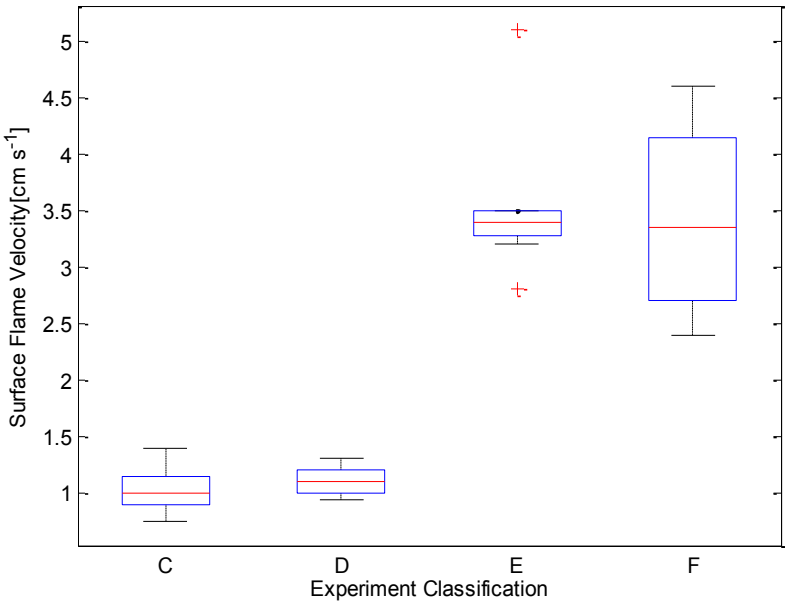

Figure 21 (b) Crown flame velocity by experiment classification. Flame velocity approximated from video analysis.

The plots of flame speed calculated from the thermocouples against the downwind distance is presented in Figure 22 and 23 for both surface and crown fuels. The terminal flame velocity is reached already at 80 cm from the ignition location.

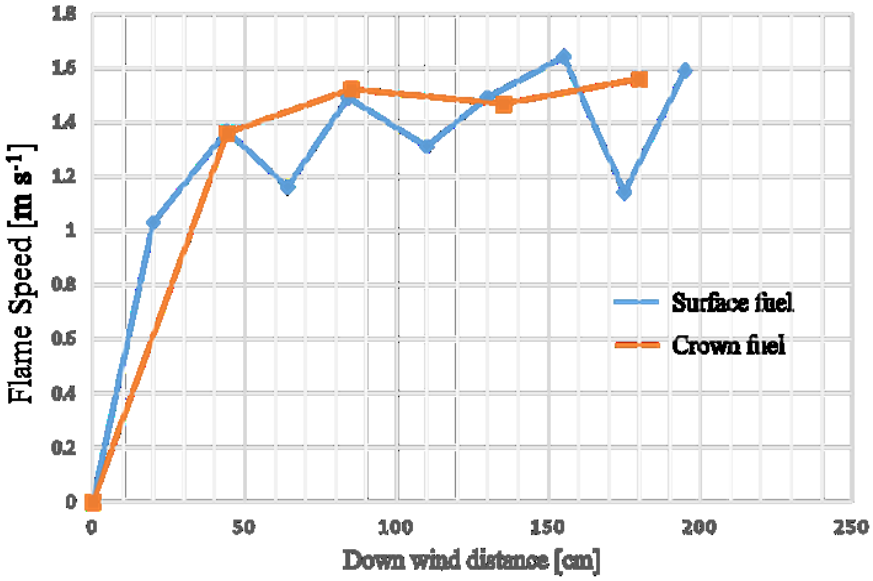

Figure 22. Flame speed calculated at the thermocouples in the crown fuel and surface fuel. The trend of active fire moves in both fuel beds is similar and at the same rate.

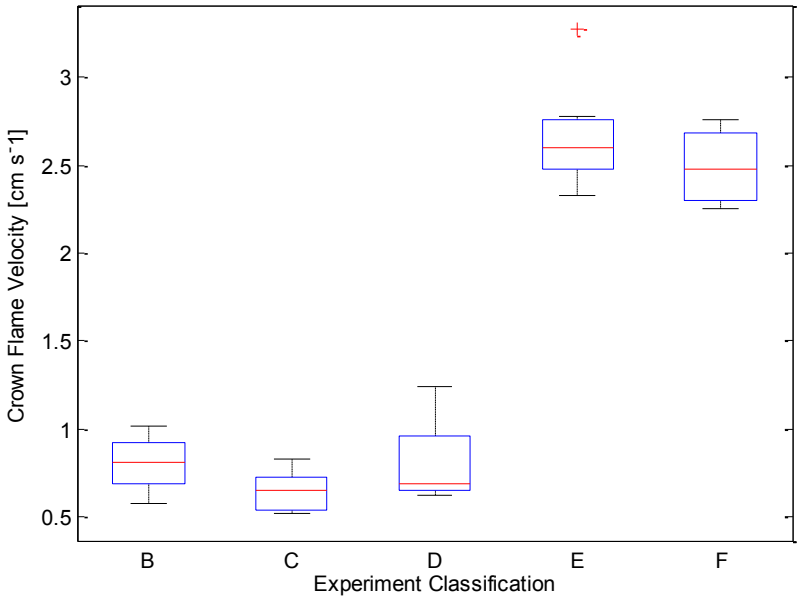

Figure 23. Crown flame velocity calculated from thermocouple data for each class.

5.1.5 Reaction Intensity

Surface fuel consumption and energy release analysis were referred to as reaction intensity in this study. The burning rate of the surface fuel was investigated and our observation revealed that the energy release rate of the fire front was produced by active flaming (85%) as well as smoldering(15%) of the organic matter in the fuels. Therefore, the rate of change of this organic matter from solid to gas is a good approximation of the subsequent heat release rate of the fire. The heat release rate per unit area can be expressed as:

$$q = H \frac{dm}{dt}, \tag{19}$$

where, q is the energy released, dm/dt is mass loss rate per unit area (fuel consumption rate), and H is the heat content of fuel, usually taken as the heat production from soft woods (21 kJ/Kg).

The reaction intensity is a function of fuel parameters including the particle size, bulk density, moisture content, and chemical composition. A plot of a mass loss versus time series during experiment 17 (class E) is given in Figure 24 while the slope of the fuel consumption for each class is presented in Figure 25.

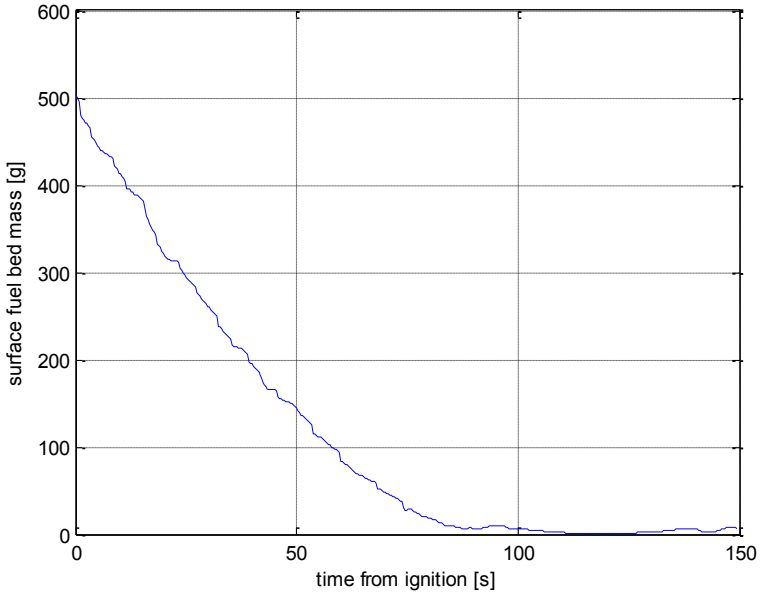

Figure 24. Surface fuel mass loss rate plot during experiment 17. Slope of the curve presents the fuel consumption rate.

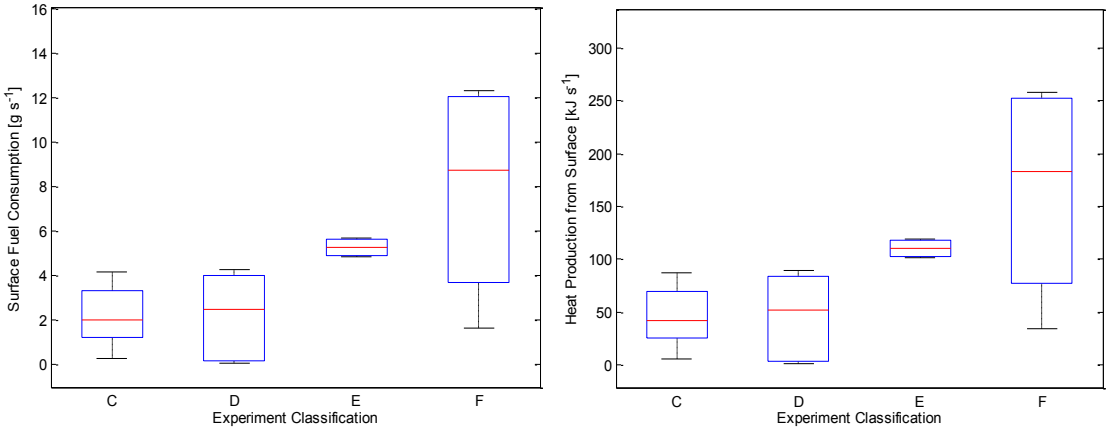

(a) (b)

Figure 25 (a) represents the fuel consumption rate, and (b) Heat production rate from surface fuel bed for each experimental class.

5.2 Results

5.2.1 Class A

The experiments under Class A focus on passive crown flame spread with no wind. Crown fuel failed to spread without the support of surface flame and wind enhanced heat transfer. The crown flames without wind are incapable of spreading. In rare cases, the crown was burning but for a short period of time. The measurements indicated a very low passive flame spread velocity of 0.4 cm s^{-1}.

5.2.2 Class B

Class B experiments had forced airflow which resulted in 100 % of crown ignition and successful crown flame spread in 78 of 100 cases. The flames became tilted due to airflow, but the median crown flame heights increase were insignificant. The crown flame velocity increased to 1.2 cm s- , three times the flame spread velocity of Class A which was 0.4 cm s-1. Wind tilted flames do better preheating of the fuel and the flaming pyrolysis gases are advected by wind towards the unburned fuels causing their ignition. Thus, the wind causes effective flame spread with a propagation velocity by a factor of 3 larger compared to no wind case.

5.2.3 Class C

Category C experiments study the interactions of surface and crown fuels at the continuous flame height (60 cm) under no wind condition. Successful Crown ignition was 78%. The crown ignition occurred when column flame structure was observed in the

crown. Once ignited, the crown flame propagates together with surface flame. Surface flame assists crown flame by preheating its fuel. The measured surface flame front velocity was approximately 1.0 cm s^{-1}. The surface fuel consumption of excelsior was approximately 2 g s^{-1} producing 50 watts of heat.

5.2.4 Class D

Experiments in this class differ from Class C experiment by changing the surface-crown fuel separation distance from 60 cm to the intermittent flame zone (70 cm). The crown fire intensity was low compared to class E and F – in 50% of experiments crown flame was not related to the surface. Failure to ignite crown fuels at the edge was observed. However, torching at mid-section of crown fuels, and backfires from torching were observed. The experiments had a greater failure to spread (50%). Surface flame rates were the same as Class C. At a greater crown height, crown fire flame velocity was considerably less from video analysis. Surface fuel consumption and heat production were the same as Class C.

5.2.5 Class E

These experiments were setup to investigate the interactions of surface and crown fuels at the continuous flame zone height (60 cm) for low wind speeds. 100% of experiments were capable to transfer flames to the crown. 22% of the experiments show passive fire characteristics and spread failure. Most cases show active flame characteristics with flames in the crown driven by surface flame front. Surface flame velocities were significantly greater by a factor 3 due to the introduction of wind. Crown flame rate also significantly

increased. Surface heat production was increased by double the value without wind (Class D).

5.2.6 Class F

Class F experiments showed similar results as Class E experiments, except for the separation distance of 70cm. Despite the fact that these experiments were designed to have intermittent flame heights, continuous flame height conditions were observed. We observed 91% of experiments successfully showing active flame properties. The flame height were slightly greater than what was observed in Class E. Similar flame velocities were observed with Class E experiments. Median crown velocities were slightly higher compared to Class E. Fuel consumption and energy production showed greater variance compared to the Class E experiments.

The general observation that was common to all classes showed that surface flame velocity depends on wind conditions and is independent of separation distance from crowns.

A Summary of statistics on failure to ignite or spread is provided in Table 3. In Figure 26, the statistics of failure to ignite or spread from Table 3 are plotted on the histogram for all the classes of the experiment.

Table 3: Summary of ignition statistics

Classification	Crown Ignition	Crown fire successful Ignition and spread
A	50%	50%
B	100%	78%
C	78%	100%
D	75%	75%
E	100%	78%
F	89%	100%

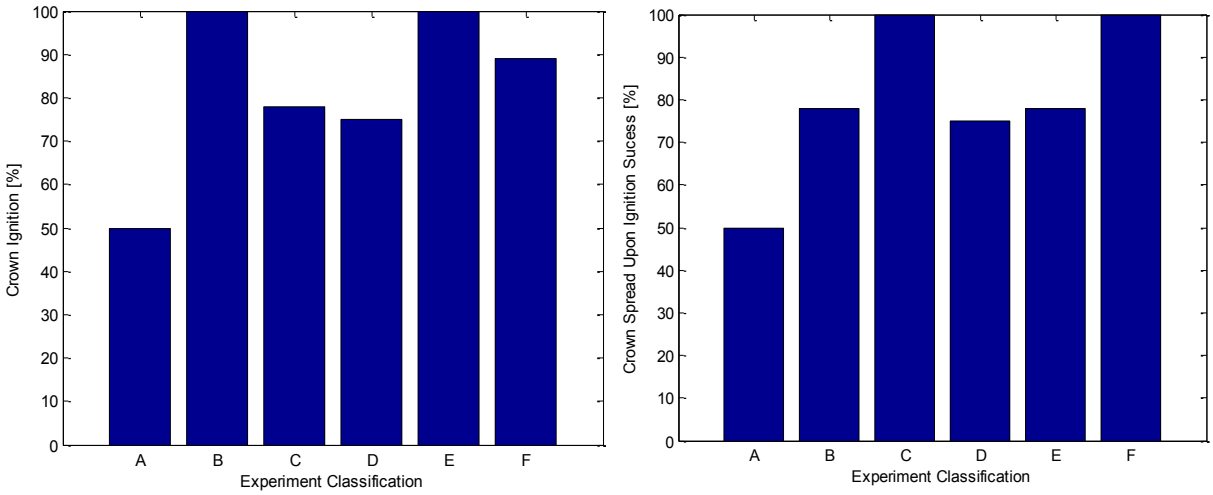

Figure 26. Histogram of Successful Crown Ignition and Crown Flame Spread for each experimental class.

6.0 Fire Dynamic Simulator Results

The sensitivity of the model predictions of mass loss rate and radiant heat flux on grid resolution and computational domain size was tested. The computational domains of the ‘‘production” runs were 3 m x 1.2 m x 1.2 m (in x, y, and z directions with z being the vertical axis). Mass loss rates and heat fluxes from simulations were recorded automatically by FDS in the excel output files. Future work will better identify the source and sensitivities of these variations in the model results which can be due to our representation of the vegetation and/or our numerical and physical modeling approaches.

Five classes of simulations - 1, 2, 3, 4, and 5, Table 4, were run on 2.6 GHz processor with 16 GB of RAM. Each simulation in a class required 177 MB of memory, 20 – 40 net CPU minutes and 8 - 40 seconds of simulated time (2300 time step).

Table 4 – Classes of FDS Simulations

Class	Surface Fuel	Crown Fuel	Hotspot on Surface	Hotspot on Crown	Hotspot Temperature(s) deg. C.
1		X	X	X	5000
2	X	X	X		5000
3	X	X	X	X	5000
4	X		X		5000
5	X	X	X		Vary, Table 9.

Estimate of the bulk densities of the vegetation were obtained from the measured surface and crown fuels distributed over the two fuel beds. It was observed that once

pyrolysis is complete, leaving only char, a fuel element remains for the duration of the simulation. The bulk density and packing ratio play an important role in the intensity of fire and heat transfer. Low bulk density allows ignition and flame spread to occur rapidly but reduces the overall heat in the surface and crown fuels.

The hot spot introduced in the simulations was held hot throughout the period of simulation for the same time the ignitor was flaming. The reason is to induce a buoyant flow of hot air on the fuels keeping the wall temperature well above 800 deg. C. This effect represent the actions of firebrands in the experimental setup. Tables 5, 6, 7, 8 and 9 show detail results of the simulations.

The results class 1 simulations which contains four experiment with crown fuel only in the presence of hot spot are in the Table 5. Surface temperature was held constant for all bulk densities. Fuel burnout time was taken for each of the simulations.

Table 5 – Simulations of only crown fuel with one hot spot (Class 1)

S/N	BULK DENSITY Kg/m3	HOT SPOT deg.C	THICKNESS (m)	HEIGHT BTW FUEL BEDS (m)	BURNOUT TIME tb (sec)	Observation on fuel	Time Summary
1	20	5000	0.2	0.7	8	left over	t1
2	15	5000	0.2	0.7	7.99	small left over	
3	10	5000	0.2	0.7	6.95	...	
4	5	5000	0.2	0.7	4.85	...	

For class 2 simulations presented in Table 6 the crown fuel height and surface temperature were held constant for all densities. But for these cases the hot spot was only on the surface fuel. The time taken for the flame to completely consume the fuel was recorded for each simulation.

Table 6 – Surface and Crown fuels with hot spot only on surface fuel (Class 2)

S/N	BULK DENSITY Kg/m3	HOT SPOT deg.C	THICKNESS (m)	HEIGHT BTW FUEL BEDS (m)	BURNOUT TIME tb (sec)	Observation on fuel	Time Summary
1	20	5000	0.2	0.7	7.99	small left over	t2
2	15	5000	0.2	0.7	7.5	...	
3	10	5000	0.2	0.7	5.7	...	
4	5	5000	0.2	0.7	4.46	...	

Class 3 simulations maintained the same conditions as in class 1and 2 simulations as shown in Table 6 but added hot spot to both surface and crown fuel. Similarly, fuel burnout time was recorded for each simulation run.

Table 7 - Surface and crown fuels with hot spot on both fuels (Class 3)

S/N	BULK DENSITY Kg/m3	HOT SPOT deg.C	THICKNESS (m)	HEIGHT BTW FUEL BEDS (m)	BURNOUT TIME tb (sec)	Observation on fuel	Time Summary
1	20	5000	0.2	0.7	7.6	...	t3
2	15	5000	0.2	0.7	6.32	...	
3	10	5000	0.2	0.7	5.51	...	
4	5	5000	0.2	0.7	4	...	

The simulations for class 4 shown in figure 8 contain surface fuel only with hot spot. Surface temperature was held constant for all bulk densities. Fuel burnout time was taken for each of the simulations.

Table 8 - Only surface fuel with hot spot (Class 4)

S/N	BULK DENSITY Kg/m3	HOT SPOT deg.C	THICKNESS (m)	HEIGHT BTW FUEL BEDS (m)	BURNOUT TIME tb (sec)	Observation on fuel	Time Summary
1	20	5000	0.2	0.7	7.98	left over	t4
2	15	5000	0.2	0.7	7.78	...	
3	10	5000	0.2	0.7	6.46	...	
4	5	5000	0.2	0.7	5.08	...	

Class 5 simulations were run with constant bulk density for all hot spot temperatures. All other conditions were the same as with class 2 simulations. The results are shown below in Table 9.

Table 9 – Simulations with increasing surface temperature (Class 5)

S/N	BULK DENSITY Kg/m3	HOT SPOT deg.C	THICKNESS (m)	HEIGHT BTW FUEL BEDS (m)	BURNOUT TIME tb (sec)	Observation on fuel	Time Summary
1	15	5000	0.2	0.7	8.65	...	t4<t3<t2<t1
2	15	6000	0.2	0.7	7.14	...	
3	15	7000	0.2	0.7	6.46	...	
4	15	8000	0.2	0.7	5.24	...	

The results in Tables 5, 6, 7, 8 and 9 showed that in FDS modelling, burning rate of solid fuels depends on some variables such as flame temperature, Bulk density and thickness, height between surface and crown fuels.

1. High temperature of the flame (hot spot temperatures) leads to a faster burning rate.
2. Burning rate is inversely proportional to the density of the solid fuel. At low density, solid fuel burns faster. The same is true for thickness.
3. Height between the surface and crow fuel is another factor that affects the ignition time and the burning rate. The higher the separating height the more time it take the flame/convective heat to reach the crown fuel. However, if the base fire plume is high enough to ignite fire on the crown, burning may start earlier than the usual time.

Keeping any of the above variables constant, it is possible to study the behavior of fire and modify the flame spread/burning rate. The most important fact still remain, in order to burn

away solid fuel, the flame must reach the ignition temperature of the fuel and be constant for 4-6 seconds for any burning to take place. The burnout time of reacting solid fuel is calculated automatically by FDS as

$$t = \frac{\rho \delta \Delta H}{q''} \tag{19}$$

where, t is the burnout time, δ is layer thickness, ΔH is the heat of combustion, ρ is material density, and q'' is the heat released.

7.0 Conclusion

We can conclude that surface flame velocity depends on wind conditions and is independent of separation distance from crowns. The separation distance between the surface fuel and crown fuel plays a significant role in fire transition from surface fuel to elevated fuel as observed in class D experiment. In this experiment, surface flame height was captured by video recording for the analysis. In addition to crown separation, crown ignition and propagation were greatly influenced by wind conditions. Crown fuel ignited quickly and burned intensely when wind was present. The flame tilted forward to preheat the adjacent fuel resulting in a large fire that would propagate fast. However, the crown flame height exceeded video frame and could not be calculated for categories C-F. Special experimental setup is needed to establish these flame heights. Since this was out of the scope of presented study such modifications are left for future work.

The results from FDS simulations also show that burnout time for simulations containing surface and crown fuels is shorter than simulations with only crown fuel or surface fuel. This is an indication that heat released by the surface fuel takes part in preheating crown fuel. Low bulk density favors faster burning rate, however the heat released was small compare to heat released from higher bulk density simulations. In FDS, problem of numerical instability occurred when we tried to run simulations with open boundary conditions. The reason for this behavior was not fully understood, however, we speculate that early termination of FDS simulation are due to too large time step. This challenge is one of the future works that will be captured so that FDS can both run under closed and open boundary conditions. The other challenge in FDS simulations is the

inability of FDS to recognize two fuels of different materials in the same simulation. The future works of this research will look into the issue in great detail.

8.0 References

Albini, F.A. Estimating Wildfire Behavior and Effects. USDA Forest Service General Technical Report INT-30, 1976.

Alexander, M.E., Cruz, M.G. Crown fire dynamics in conifer forests in synthesis of knowledge of extreme fire behavior for fire managers, volume 1, USDA Forest Service, Pacific Northwest. Research Station, Gen. Tech. Rep. PNWGTR-854, Portland, OR, Chapter 8, pages 107-142.

Andrews, P.L. BEHAVE: Fire Behavior Prediction and Fuel Modeling System, BURN - Subsystem, Part 1. USDA Forest Service General Technical Report INT-194.

Babrauskas, V. Common solids, Ignition Handbook. Fire Science Publishers, Issaquah, WA, Chap. 7, 2003.

Bilger, R. Computational Field Model in Fire Research and Engineering Procedures, Forth Internal Symposium, Fire Safety Science, pp 95 – 110, June 1994.

Buchanan, A. Fire Engineering Design Guide, Center for Advanced Engineering, New Zealand, 2001.

Byram, G.M., Davis, K.P. Combustion of forest fuels in Forest Fire: Control and Use, McGraw-Hill, New York, Chap. 3, 1959.

Carl D. Wren, Ezekoye O. A. FDS-Smokeview Models Struggles and Triumphs in Public Safety Application and Scientific Perspectives. Austin Fire Department, Engineering Services Section and University of Texas, Mechanical Engineering Department, USA, 2006.

Cox, P. 'Basic Considerations', Combustion Fundamentals of Fire, Ed. G. Cox Academic Press, London, 1995.

Engstrom, D., Butler, J. K., Smith, S. G., Baxter, L. L., Fletcher, T. H., and Weise, D. R. Ignition behavior of Live California Chaparral Leaves, Combustion Science and Technology, 176:9, 1577-1591, 2010.

FDS-SMV Official Website. Found at: http://www.fire.nist.gov/fds/. Last Updated November, 2013.

Finney, M. A. FARSITE: Fire Area Simulator-Model Development and Evaluation, USDA Forest Service Research paper RMRS-RP-4, March 1998.

Floyd, J., Baulm, H., McGratten, K. A mixture fraction combustion model for fire simulation using CFD, The International Conference on Engineered Fire Protection Design, pages 279 – 290, 2001.
Fosberg, M. and Deeming, J. E. Derivation of the 1-hour and 10-hour Time lag, Fuel Moisture Calculations for Fire-Danger Rating. USDA Forest Service. Note RM-207, Rocky Mountain Forest and Range Experiment Station, Fort Collins, CO., 1971.

Hume, B. Water Mist Suppression in Conjunction with Displacement Ventilation, Fire Engineering Research Report, University of Canterbury, New Zealand, 2003.

Joe H. Scott; Robert E. Burgan. Standard Fire Behavior Fuel Models: A Comprehensive Set for Use with Rothermel's Surface Fire Spread Model, USDA Forest Service, General Technical Report RMRS - GTR-153, June 2005.

Karlsson, B. and Quintiere, J. Enclosure Fire Dynamics, CRC Press, Boca Raton, Florida, 2000.

Mawhinney, N., Galea, E.R., Hoffman, N. and Patel, M.K. A critical Comparison of a Phonetics Based Fire Field Model with Experimental Compartment Fire Data, Journal of Fire Protection Engineering, 6, 137 –152, 1994.

McGrattan, K., Baum, H., Rehm, R., Hamins, A., Forney, G., Hostikka, S. Fire Dynamics Simulator (Version 3) – Technical Reference Guide, NISTIR 6783, NIST, Gaithersburg, Maryland, USA, 2002.

McGrattan, K., Hostikka, S., Floyd, J., et al. Fire Dynamics Simulator (Version 6) Technical Reference Guide Volume 1: Mathematical Model, NIST Special Publication 1018-6, November 4, 2013.

Nelson, H. Phlogiston to Computational Fluid Dynamics, Society of Fire Protection Engineering Magazine, pages 9 – 17, Winter 2002.

Petterson, N. Assessing the Feasibility of Reducing the Grid Resolution in FDS Field Modeling, Fire Engineering Research Report, University of Canterbury, New Zealand, Forest Service Research Paper INT-115, 2002.

Smardz, P. Validation of Fire Dynamics Simulator (FDS) for forced and natural convection flows, October 2006.

Sutula, J. Fire Dynamic Simulator in Fire Protection Engineering Consulting, Society of Fire Protection Engineering Magazine, pages 33 – 44, Spring 2002.

Van Wagner, C.E., Can. J. Height of crown scorch in forest fires. Forest Res., pages 3, 373–378.

Appendix A – FDS Input File

1. ***Sample of FDS Input File for Surface and crown Fuel*s with Hot Spots on both Fuels**

The first line of the input files names the output file. The title section does not take part in the simulation, but is intended to give a short description of the input file.

&HEAD CHID='SOLID_FUEL_BURN_AWAY', TITLE = 'BURN_AWAY_Test_File' /

The solid fuels are charred away by the high thermal radiation from hot spot. The gas species is mixture fraction fuel.

The next line describes the quantity of cells to be used in the computational domain. For the input file used here there are 20 cells in the X direction, 20 in the Y direction and 20 in the Z direction. The physical size of the domain is 2 m long, 2 m wide and 2 m high. An example grid size of 100 cm x 100 cm x 100 cm was used for the simulation file detailed here.

&MESH IJK=20, 20, 20 XB=0.0, 1.0, 0.0, 1.0, 0.0, 1.0 /

The next input line defined the maximum time it would take the simulation to run completely.

In the case of this simulation the maximum time was 8 seconds.

&TIME T_END=8 /

&MATL ID = 'CORN_STOVER'

HEAT_OF_REACTION = 900.

CONDUCTIVITY = 0.2

SPECIFIC_HEAT = 1.3

DENSITY = 20.

N_REACTIONS = 1

NU_SPEC = 1.

SPEC_ID = 'ASH'

REFERENCE_TEMPERATURE = 500.

HEAT_OF_COMBUSTION (1) = 45000. /

SURF ID = 'CORN_STOVER_FIELD'

COLOR = 'BROWN'

MATL_ID = 'CORN_STOVER'

THICKNESS = 0.04

BURN_AWAY = .TRUE.

BACKING = 'EXPOSED' /

&REAC FUEL='ASH', C=5, AUTO_IGNITION_TEMPERATURE=3000. /

&DUMP SMOKE3D=.TRUE. MASS_FILE=.TRUE. /

&SURF ID = 'HOT' TMP_FRONT = 5000. COLOR = 'RED' /

FDS input file specified the positions and dimensions through the OBST lines. The obstructions are constructed by inputting a set of coordinates that describe a rectangular object. For the purposes of Smokeview a color can be specified to an object, brown in our case, this is done by the

COLOR = BROWN prompt.

&OBST XB=0.40, 0.80, 0.40, 0.80, 0.0, 0.052, SURF_ID='CORN_STOVER_FIELD' /BASE

&OBST XB=0.40, 0.80, 0.40, 0.80, 0.28, 0.34, SURF_ID='CORN_STOVER_FIELD' /CROWN

&OBST XB=0.40, 0.45, 0.40, 0.80, 0.052, 0.092, SURF_ID='HOT'/

&OBST XB=0.40, 0.435, 0.40, 0.80, 0.34, 0.39, SURF_ID='HOT'/

&BNDF QUANTITY='WALL TEMPERATURE' /

&BNDF QUANTITY='BURNING RATE' /

&BNDF QUANTITY='NET HEAT FLUX' /

The SLCF lines describe the slice files for temperature and gas velocity. A slice file contains data (temperature and velocity) measured within a rectangular array of grid points at each recorded time steps. Continuously shaded contours are drawn for simulation quantities.

&SLCF PBX=0.5, QUANTITY='TEMPERATURE' /

&SLCF PBX=0.5, QUANTITY='INTEGRATED INTENSITY' /

&SLCF PBX=0.5, QUANTITY='MASS FRACTION', SPEC_ID='ASH' /

&SLCF PBY=0.5, QUANTITY='TEMPERATURE' /

&SLCF PBY=0.5, QUANTITY='INTEGRATED INTENSITY' /

&SLCF PBY=0.5, QUANTITY='MASS FRACTION', SPEC_ID='ASH' /

&SLCF PBZ=0.5, QUANTITY='TEMPERATURE' /

&SLCF PBZ=0.5, QUANTITY='INTEGRATED INTENSITY' /

&SLCF PBZ=0.5, QUANTITY='MASS FRACTION', SPEC_ID='ASH' /

&DEVC XB = 0, 1, 0, 1, 0, 1, QUANTITY = 'DENSITY', SPEC_ID='ASH',

STATISTICS = 'VOLUME INTEGRAL' ID = 'Mass fuel'/

&DEVC XB = 0, 1, 0,1,0,1, QUANTITY = 'HRR' ID = 'HRR' /

/&DEVC XB = 0.30, 0.70, 0.0, 1.0, 0.30, 0.70, STATISTICS = 'SURFACE INTEGRAL',

QUANTITY = 'SURFACE DENSITY', ID = 'Mass solid' /

&TAIL /

See figures 4-7 for Smokeview image.

2. ***Sample of FDS Input File for Surface and crown Fuel*s with Hot Spots on Surface Fuel**

&HEAD CHID='SOLID_FUEL_BURN_AWAY ', TITLE='BURN_AWAY_Test_File' /

The solid fuels are charred away by the high thermal radiation from hot spot. The mass of the fuel is 0.2 * 0.2^2 m3 * 20 kg/m3 = 0.16 kg.

This should be compared to the final value of fuel density volume integral, computed by the first DEVC.

The gas species is mixture fraction fuel.

&MESH IJK=20, 20, 20 XB=0.0,1.0,0.0,1.0,0.0,1.0 /

&TIME T_END=8, DT = 0.05, /

&MATL ID = 'CORN_STOVER'

HEAT_OF_REACTION = 900.

CONDUCTIVITY = 0.2

SPECIFIC_HEAT = 1.3

DENSITY = 20.

N_REACTIONS = 1

NU_SPEC = 1.

SPEC_ID = 'ASH'

REFERENCE_TEMPERATURE = 500.

HEAT_OF_COMBUSTION(1) = 45000./

&SURF ID = 'CORN_STOVER_FIELD'

COLOR = 'BROWN'

```
    MATL_ID          = 'CORN_STOVER'
    THICKNESS         =  0.04
    BURN_AWAY          = .TRUE.
    BACKING           = 'EXPOSED' /
&REAC FUEL='ASH', C=5, AUTO_IGNITION_TEMPERATURE=3000. /
&DUMP SMOKE3D=.TRUE., MASS_FILE=.TRUE. /
&SURF ID = 'HOT' TMP_FRONT = 5000., COLOR = 'RED' /
&OBST     XB=0.40,0.80,0.40,0.80,0.0,0.052,     SURF_ID='CORN_STOVER_FIELD'
/BASE
&OBST     XB=0.40,0.80,0.40,0.80,0.28,0.34,     SURF_ID='CORN_STOVER_FIELD'
/CROWN
&OBST XB=0.40,0.45,0.40,0.80,0.052,0.092, SURF_ID='HOT'/
&BNDF QUANTITY='WALL TEMPERATURE' /
&BNDF QUANTITY='BURNING RATE' /
&BNDF QUANTITY='NET HEAT FLUX' /
&SLCF PBX=0.5, QUANTITY='TEMPERATURE' /
&SLCF PBX=0.5, QUANTITY='INTEGRATED INTENSITY' /
&SLCF PBX=0.5, QUANTITY='MASS FRACTION',SPEC_ID='ASH' /
&SLCF PBY=0.5, QUANTITY='TEMPERATURE' /
&SLCF PBY=0.5, QUANTITY='INTEGRATED INTENSITY' /
&SLCF PBY=0.5, QUANTITY='MASS FRACTION',SPEC_ID='ASH' /
&SLCF PBZ=0.5, QUANTITY='TEMPERATURE' /
```

```
&SLCF PBZ=0.5, QUANTITY='INTEGRATED INTENSITY' /
&SLCF PBZ=0.5, QUANTITY='MASS FRACTION',SPEC_ID='ASH' /
&DEVC XB = 0,1,0,1,0,1, QUANTITY = 'DENSITY',SPEC_ID='ASH',
STATISTICS = 'VOLUME INTEGRAL' ID = 'Mass fuel'/
&DEVC XB = 0,1,0,1,0,1, QUANTITY = 'HRR' ID = 'HRR' /
&DEVC XB = 0.30,0.70,0.0,1.0,0.30,0.70, STATISTICS = 'SURFACE INTEGRAL',
QUANTITY = 'SURFACE DENSITY', ID = 'Mass solid' /
&TAIL /
```

3. *Sample of FDS Input File for Crown Fuel*s with Hot Spots

```
&HEAD CHID='SOLID_FUEL_BURN_AWAY CROWN', TITLE='BURN AWAY Test
File' /
The Crown fuel is charred away by the high thermal radiation
from hot spot. The mass of the box is 0.2 * 0.2^2 m3 * 20 kg/m3 = 0.16 kg.
This should be compared to the final value of fuel density volume integral,
computed by the first DEVC.
The gas species is mixture fraction fuel.
&MESH IJK=20, 20, 20 XB=0.0,1.0,0.0,1.0,0.0,1.0 /
&TIME T_END=8, DT = 0.05, /
&MATL ID              = 'CORN_STOVER'
HEAT_OF_REACTION      = 900.
CONDUCTIVITY          = 0.2
SPECIFIC_HEAT         = 1.3
DENSITY               = 20.
N_REACTIONS           = 1
NU_SPEC               = 1.
SPEC_ID               = 'ASH'
REFERENCE_TEMPERATURE     = 500.
HEAT_OF_COMBUSTION(1)     = 45000./
&SURF ID              = 'CORN_STOVER_FIELD'
    COLOR             = 'BROWN'
```

```
    MATL_ID           = 'CORN_STOVER'
    THICKNESS       = 0.04
    BURN_AWAY          = .TRUE.
    BACKING            = 'EXPOSED' /
&REAC FUEL='ASH', C=5, AUTO_IGNITION_TEMPERATURE=3000. /
&DUMP SMOKE3D=.TRUE., MASS_FILE=.TRUE. /
&SURF ID = 'HOT' TMP_FRONT = 5000., COLOR = 'RED' /
&OBST      XB=0.40,0.80,0.40,0.80,0.28,0.34,      SURF_ID='CORN_STOVER_FIELD'
/CROWN
&OBST XB=0.40,0.435,0.40,0.80,0.34,0.39, SURF_ID='HOT'/
&BNDF QUANTITY='WALL TEMPERATURE' /
&BNDF QUANTITY='BURNING RATE' /
&BNDF QUANTITY='NET HEAT FLUX' /
&SLCF PBX=0.5, QUANTITY='TEMPERATURE' /
&SLCF PBX=0.5, QUANTITY='INTEGRATED INTENSITY' /
&SLCF PBX=0.5, QUANTITY='MASS FRACTION',SPEC_ID='ASH' /
&SLCF PBY=0.5, QUANTITY='TEMPERATURE' /
&SLCF PBY=0.5, QUANTITY='INTEGRATED INTENSITY' /
&SLCF PBY=0.5, QUANTITY='MASS FRACTION',SPEC_ID='ASH' /
&SLCF PBZ=0.5, QUANTITY='TEMPERATURE' /
&SLCF PBZ=0.5, QUANTITY='INTEGRATED INTENSITY' /
&SLCF PBZ=0.5, QUANTITY='MASS FRACTION',SPEC_ID='ASH' /
```

```
&DEVC XB = 0,1,0,1,0,1, QUANTITY = 'DENSITY',SPEC_ID='ASH',
STATISTICS = 'VOLUME INTEGRAL' ID = 'Mass fuel'/
&DEVC XB = 0,1,0,1,0,1, QUANTITY = 'HRR' ID = 'HRR' /
/&DEVC XB = 0.30,0.70,0.0,1.0,0.30,0.70, STATISTICS = 'SURFACE INTEGRAL',
QUANTITY = 'SURFACE DENSITY', ID = 'Mass solid' /
&TAIL /
```

4. *Sample of FDS Input File for Surface Fuel* with Hot Spots

```
&HEAD CHID='SOLID_FUEL_BURN_AWAY CROWN',
TITLE='BURN_AWAY_Surface /
The surface fuel is charred away by the high thermal radiation from hot spot. The mass of
the box is 0.2 * 0.2^2 m3 * 20 kg/m3 = 0.16 kg.
This should be compared to the final value of fuel density volume integral, computed by
the first DEVC.
The gas species is mixture fraction fuel.
&MESH IJK=20, 20, 20 XB=0.0,1.0,0.0,1.0,0.0,1.0 /
&TIME T_END=8, DT = 0.05, /
&MATL ID              = 'CORN_STOVER'
HEAT_OF_REACTION      = 900.
CONDUCTIVITY          = 0.2
SPECIFIC_HEAT         = 1.3
DENSITY               = 20.
N_REACTIONS           = 1
NU_SPEC               = 1.
SPEC_ID               = 'ASH'
REFERENCE_TEMPERATURE     = 500.
HEAT_OF_COMBUSTION(1)     = 45000./
&SURF ID              = 'CORN_STOVER_FIELD'
    COLOR             = 'BROWN'
```

```
    MATL_ID            = 'CORN_STOVER'
    THICKNESS          =  0.04
    BURN_AWAY          = .TRUE.
    BACKING            = 'EXPOSED' /
&REAC FUEL='ASH', C=5, AUTO_IGNITION_TEMPERATURE=3000. /
&DUMP SMOKE3D=.TRUE., MASS_FILE=.TRUE. /
&SURF ID = 'HOT' TMP_FRONT = 5000., COLOR = 'RED' /
&OBST      XB=0.40,0.80,0.40,0.80,0.0,0.052,      SURF_ID='CORN_STOVER_FIELD'
/BASE
&OBST XB=0.40,0.45,0.40,0.80,0.052,0.092, SURF_ID='HOT'/
&BNDF QUANTITY='WALL TEMPERATURE' /
&BNDF QUANTITY='BURNING RATE' /
&BNDF QUANTITY='NET HEAT FLUX' /
&SLCF PBX=0.5, QUANTITY='TEMPERATURE' /
&SLCF PBX=0.5, QUANTITY='INTEGRATED INTENSITY' /
&SLCF PBX=0.5, QUANTITY='MASS FRACTION',SPEC_ID='ASH' /
&SLCF PBY=0.5, QUANTITY='TEMPERATURE' /
&SLCF PBY=0.5, QUANTITY='INTEGRATED INTENSITY' /
&SLCF PBY=0.5, QUANTITY='MASS FRACTION',SPEC_ID='ASH' /
&SLCF PBZ=0.5, QUANTITY='TEMPERATURE' /
&SLCF PBZ=0.5, QUANTITY='INTEGRATED INTENSITY' /
&SLCF PBZ=0.5, QUANTITY='MASS FRACTION',SPEC_ID='ASH' /
```

```
&DEVC XB = 0,1,0,1,0,1, QUANTITY = 'DENSITY',SPEC_ID='ASH',
STATISTICS = 'VOLUME INTEGRAL' ID = 'Mass fuel'/
&DEVC XB = 0,1,0,1,0,1, QUANTITY = 'HRR' ID = 'HRR' /
/&DEVC XB = 0.30,0.70,0.0,1.0,0.30,0.70, STATISTICS = 'SURFACE INTEGRAL',
QUANTITY = 'SURFACE DENSITY', ID = 'Mass solid' /
&TAIL /
```

Appendix B - FDS Input File Special Cases

Special Case 1: Dual Fuels - Crown Ignition Failure

*Sample of FDS Input File for Surface and crown Fuel*s with Hot Spots on both Fuels

```
&HEAD CHID='SOLID_FUEL_BURN_AWAY', TITLE='BURN_AWAY_Test_File' /
The solid fuel is charred away by the high thermal radiation
from hot spot. The mass of the fuel is  2.28 * 0.8 * 0.1 m3 *3 kg/m3 = 0.5kg.And the
second solid fuel is 1.82 * 0.62 * 0.2 m3 *9.2 kg/m3 = 2kg.
This should be compared to the final value of fuel density volume integral,
computed by the first DEVC.
The gas species is mixture fraction fuel.
&MESH IJK=20,20,20 XB=0.0,3.0,0.0,1.2,0.0,1.2 /
&TIME T_END=40 /
&MATL ID              = 'DRIED_WOOD_SHAVINGS'
HEAT_OF_REACTION              = 900.
CONDUCTIVITY                  = 0.2
SPECIFIC_HEAT                 = 1.3
DENSITY                       = 3.
N_REACTIONS                   = 1.
NU_SPEC                       = 1.
SPEC_ID                       = 'ASH'
REFERENCE_TEMPERATURE     = 500.
```

HEAT_OF_COMBUSTION(1) = 45000./

&MATL ID = 'GREEN_VEGITATION'

HEAT_OF_REACTION = 950.

CONDUCTIVITY = 0.2

SPECIFIC_HEAT = 1.3

DENSITY = 9.

N_REACTIONS = 1.

REFERENCE_TEMPERATURE = 700.

HEAT_OF_COMBUSTION(1) = 45000./

&SURF ID = 'DRIED_WOOD_SHAVINGS_SURFACE'

COLOR = 'BROWN'

MATL_ID = 'DRIED_WOOD_SHAVINGS'

THICKNESS = 0.04

BURN_AWAY = .TRUE.

BACKING = 'EXPOSED' /

&SURF ID = 'GREEN_VEGETATION_CROWN'/

COLOR = 'GREEN'

MATL_ID = 'GREEN_VEGETATION'

THICKNESS = 0.04

BURN_AWAY = .TRUE.

BACKING = 'EXPOSE' /

&REAC FUEL='ASH', C=5, AUTO_IGNITION_TEMPERATURE=3000. /

```
&DUMP SMOKE3D=.TRUE., MASS_FILE=.TRUE. /

&SURF ID = 'HOT' TMP_FRONT = 5000., COLOR = 'RED' /

&OBST XB= 0.5, 2.28, 0.2, 1.0, 0.0, 0.10, SURF_ID=

'DRIED_WOOD_SHAVINGS_SURFACE' / Surface

&OBST XB=0.5,2.32,0.319,0.939,0.70,0.9,

SURF_ID='GREEN_VEGETATION_CROWN'/ Crown

&OBST XB=0.5,0.55,0.20,1.0,0.10,0.16, SURF_ID='HOT'/

/&OBST XB=0.5,0.55,0.319,0.939,0.90,0.95, SURF_ID='HOT', /CROWN

&BNDF QUANTITY='WALL TEMPERATURE' /

&BNDF QUANTITY='BURNING RATE' /

&BNDF QUANTITY='NET HEAT FLUX' /

&SLCF PBX=0.5, QUANTITY='TEMPERATURE' /

&SLCF PBX=0.5, QUANTITY='INTEGRATED INTENSITY' /

&SLCF PBX=0.5, QUANTITY='MASS FRACTION',SPEC_ID='ASH' /

&SLCF PBY=0.5, QUANTITY='TEMPERATURE' /

&SLCF PBY=0.5, QUANTITY='INTEGRATED INTENSITY' /

&SLCF PBY=0.5, QUANTITY='MASS FRACTION',SPEC_ID='ASH' /

&SLCF PBZ=0.5, QUANTITY='TEMPERATURE' /

&SLCF PBZ=0.5, QUANTITY='INTEGRATED INTENSITY' /

&SLCF PBZ=0.5, QUANTITY='MASS FRACTION',SPEC_ID='ASH' /

&DEVC XB = 0,1,0,1,0,1, QUANTITY = 'DENSITY',SPEC_ID='ASH',

STATISTICS = 'VOLUME INTEGRAL' ID = 'Mass fuel'/
```

```
&DEVC XB = 0,1,0,1,0,1, QUANTITY = 'HRR' ID = 'HRR' /
/&DEVC XB = 0.30,0.70,0.0,1.0,0.30,0.70, STATISTICS = 'SURFACE INTEGRAL',
QUANTITY = 'SURFACE DENSITY', ID = 'Mass solid' /
&TAIL /
```

Special Case 2: Same Fuels - Fuels Burn Away

*Sample of FDS Input File for Surface and crown Fuel*s with Hot Spots on Surface Fuel.

&HEAD CHID='SOLID_FUEL_BURN_AWAY', TITLE='BURN_AWAY_Test_File' /

The Solid fuel is charred away by the high thermal radiation

from hot spot. The mass of the fuel is 2.28 * 0.8 * 0.1 m3 *3 kg/m3 = 20kg. And the

second solid fuel is 1.82 * 0.62 * 0.2 m3 *20 kg/m3 = 2kg.

This should be compared to the final value of fuel density volume integral,

computed by the first DEVC.

The gas species is mixture fraction fuel.

&MESH IJK=30,30,30 XB=0.0,3.0,0.0,1.2,0.0,1.2 /

&TIME T_END=40 /

&MATL ID = 'DRIED_WOOD_SHAVINGS'

HEAT_OF_REACTION = 900.

CONDUCTIVITY = 0.2

SPECIFIC_HEAT = 1.3

DENSITY = 20.

N_REACTIONS = 1.

NU_SPEC = 1.

SPEC_ID = 'ASH'

REFERENCE_TEMPERATURE = 500.

HEAT_OF_COMBUSTION(1) = 45000./

```
&SURF ID                = 'DRIED_WOOD_SHAVINGS'
    COLOR               = 'BROWN'
    MATL_ID             = 'CORN_STOVER'
    THICKNESS           =  0.04
    BURN_AWAY           = .TRUE.
    BACKING             = 'EXPOSED' /
&REAC FUEL='ASH', C=5, AUTO_IGNITION_TEMPERATURE=3000. /
&DUMP SMOKE3D=.TRUE., MASS_FILE=.TRUE. /
&SURF ID = 'HOT' TMP_FRONT = 5000., COLOR = 'RED' /
&OBST XB=0.5, 2.28, 0.2, 1.0, 0.0, 0.10, SURF_ID= 'DRIED_WOOD_SHAVINGS'/
Surface
&OBST XB=0.5,2.32,0.319,0.939,0.70,0.9, SURF_ID='DRIED_WOOD_SHAVINGS'/
Crown
&OBST XB=0.5,0.55,0.20,1.0,0.10,0.16, SURF_ID='HOT'/
/&OBST XB=0.5,0.55,0.319,0.939,0.90,0.95, SURF_ID='HOT'/CROWN
&BNDF QUANTITY='WALL TEMPERATURE' /
&BNDF QUANTITY='BURNING RATE' /
&BNDF QUANTITY='NET HEAT FLUX' /

&SLCF PBX=0.5, QUANTITY='TEMPERATURE' /
&SLCF PBX=0.5, QUANTITY='INTEGRATED INTENSITY' /
```

```
&SLCF PBX=0.5, QUANTITY='MASS FRACTION',SPEC_ID='ASH' /
&SLCF PBY=0.5, QUANTITY='TEMPERATURE' /
&SLCF PBY=0.5, QUANTITY='INTEGRATED INTENSITY' /
&SLCF PBY=0.5, QUANTITY='MASS FRACTION',SPEC_ID='ASH' /
&SLCF PBZ=0.5, QUANTITY='TEMPERATURE' /
&SLCF PBZ=0.5, QUANTITY='INTEGRATED INTENSITY' /
&SLCF PBZ=0.5, QUANTITY='MASS FRACTION',SPEC_ID='ASH' /
&DEVC XB = 0,1,0,1,0,1, QUANTITY = 'DENSITY',SPEC_ID='ASH',
STATISTICS = 'VOLUME INTEGRAL' ID = 'Mass fuel'/
&DEVC XB = 0,1,0,1,0,1, QUANTITY = 'HRR' ID = 'HRR' /
/&DEVC XB = 0.30,0.70,0.0,1.0,0.30,0.70, STATISTICS = 'SURFACE INTEGRAL',
QUANTITY = 'SURFACE DENSITY', ID = 'Mass solid' /
&TAIL /
```